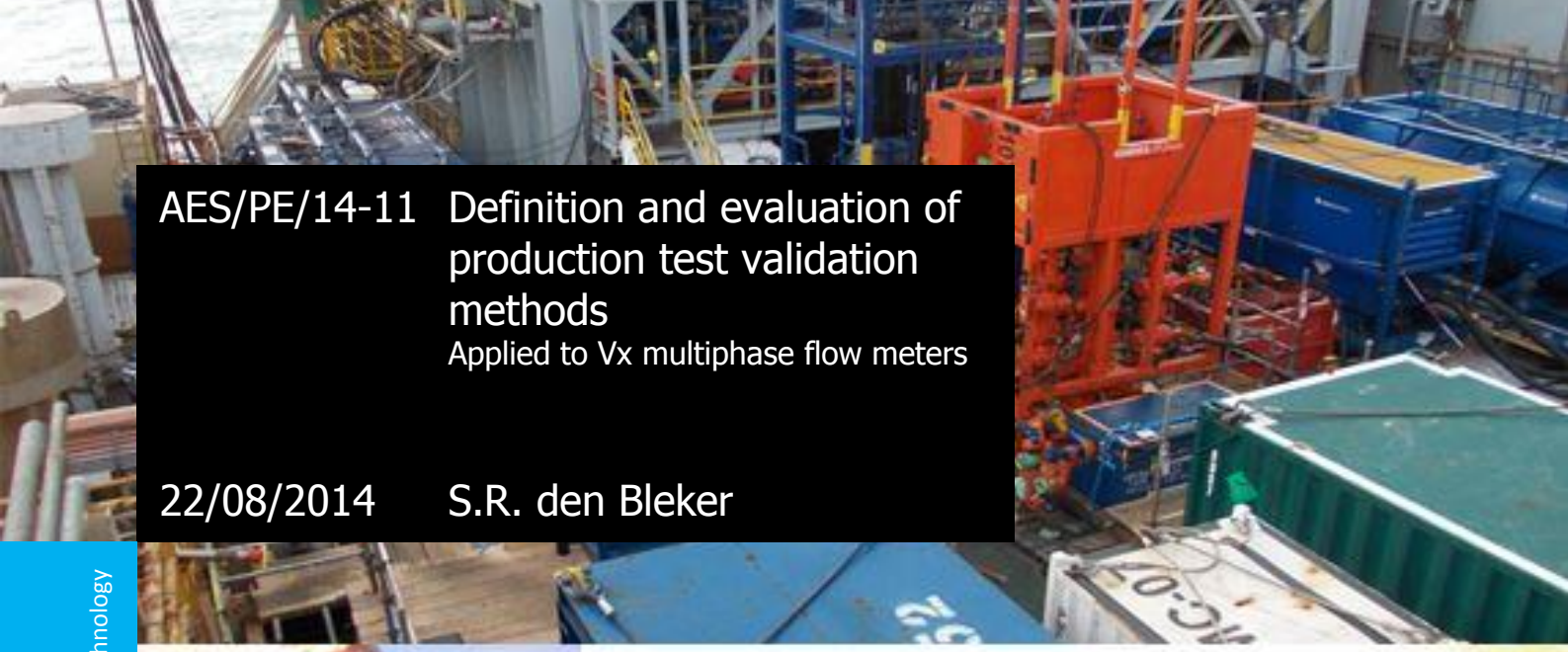

AES/PE/14-11 Definition and evaluation of production test validation methods

Applied to Vx multiphase flow meters

22/08/2014 S.R. den Bleker

Delft University of Technology

TU Delft Delft University of Technology

Challenge the future

Title	:	Definition and evaluation of production test validation methods applied to Vx multiphase flowmeters
Author	:	S.R. den Bleker,
Date	:	August 2014
Supervisor	:	Prof. dr. ir. J.D. Jansen,
Committee	:	Prof. dr. ir. R.A.W.M. Henkes, MSc. D.V. Amaral, Da Silva Dr. F. Hollaender,
TA Report number	:	AES/PE/14-11
Postal address	:	Section for Petroleum Engineering Department of Geoscience & Engineering Delft University of Technology P.O. Box 5028 The Netherlands
Telephone	:	(31) 15 2781328 (secretary)
Telefax	:	(31) 15 2781189

TU Delft Delft University of Technology

ACKNOWLEDGMENTS

This thesis has been written in collaboration with the company Schlumberger, this gave me a unique combination of practical research, field exposure and professional experiences. I very much appreciate the opportunity Schlumberger gave me.

I want to thank Yakov Shumakov for his direct guidance, time, great advises and for making this graduation internship possible. I want to thank Florian Hollaender for his time, the interesting discussions and for defining the interesting thesis topic after I expressed my interest in multiphase flow. It is very satisfying that the results of this work are actually going to be implemented. I want to thank Rafael Fejervary for helping me with all office related questions and Alistair Cowie for organizing the field jobs where I got the opportunity to get some oilfield exposure.

I want to thank Prof. Jan Dirk Jansen for his guidance and comments which helped me to have a continuous progress. I also want to thank Daniel Victor for his comments and help.

Finally, I want to thank all my friends, who had to endure countless conversations about my thesis, which was a big part of my life for the last 9 months.

S.R. den Bleker
Delft, August 2014

ABSTRACT

Accurate flow rate measurements are very important in production testing. Originally small and insignificant deviations could propagate in subsequent applications where flow rate data is used as input parameter. Vx multiphase flow meters give much more information compared to conventional test separators. This extra data can be used for extra flow rate validation on the measurements, in order to find out whether it is possible to make sense of the data and if it is applicable on the long term and viable for further applications.

Firstly, a comprehensive literature review has been done on current existing validation methods which gave a coherent overview. This work was used to define methods to detect measurement issues which can occur during a production test, defined by experts with considerable field experience.

An adjusted choke model is presented which could be run in series with a Vx meter, which is able to detect: a drift in the differential pressure sensor; the under- or overestimation of the calculated gas rate or whether the meter is operating within the designed operation envelope or not. The choke model is tested on 96 data points from actual production tests with satisfactory results for fixed choke data.

In addition, a methodology is developed to detect whether a production test has become stable or not. The method is translated into an algorithm which can be run on Vx meter output to decide in an automated fashion if a production test can be concluded, yielding representative production data. The method is tested on 700 production tests in order to define the model thresholds, which showed that the majority of the tests could have been concluded earlier. It has been found that by analyzing the statistical properties of the data it is possible to observe flow pattern transition. Furthermore, by representing certain parameters in the frequency domain, slug flow regimes can be detected and the corresponding slug flow periodicity can easily be subtracted from the data.

CONTENTS

1

INTRODUCTION

Flow rate measurements have always been essential for the petroleum industry. With accurate flow rate measurements, engineers should be able to make the right decisions throughout the whole lifespan of a well. The drilling engineer who needs an optimal mud flow rate for operating his mud motor, the completion engineer who needs accurate well test data for designing a production completion, the production engineer monitoring a well for production enhancement or the reservoir engineer who uses production data for the material balance and decline curve analyses are just a few examples. It is clear that flow rate data is used in numerous applications.

Wrong or misleading flow measurements could end up worse than one initially could expect. Originally small and insignificant flow rate data deviations could propagate in subsequent applications where flow rate data are used as input parameter. For operating companies it can, for example, end up in reputation loss which means difficulties with obtaining future licenses. Or it could result in potentially missed income by inefficient designed surface installations or artificial lift solutions.

Currently, there are countless ways available to measure the flow rate. The most common measure principles used in the petroleum industry are by measuring the mass (i.e. coriolis meter), velocity (i.e. turbine meter), positive displacement (i.e. oval gear meter) or differential pressure (i.e. orifice, venturi or v-cone meter) of the flow (Miller [1]). Most of those flow rate measurement devices could only be used for certain fluid phase(es), meters installed downstream of a test separator is a common solution for measuring multiphase flows. Some flow rate meter devices cross correlated with other techniques , such as density measurements, can measure multiphase flow without separation (Corneliussen *et al.* [2]). Whatsoever the method of measuring the flow rate, the meter is always restricted to a specific production envelope. Furthermore, there are many factors which can influence a meter. The meter could be damaged or affected by deposition of hydrates or scales for instance. A wrongly timed duration of a production test can lead to inaccurate data. Wrong user input in fluid properties for instance could affect the cross correlations in a flow computer. All in all, a meter and all the other elements involved in a production test could work expected as per standard; however, with losing the focus on other factors involved, a test still can result in what has been introduced in literature as a "successful failure" (Sikandar *et al.* [3, 4]).

Unfortunately, despite the awareness on the importance of accurate flow rate measurements, most production tests are still performed in a disorderly fashion (Ojukwu and Edwards [5]). As an extensive amount of factors could influence the flow rate measurements, (see table 1 in:Theuveny and Mehdizadeh [6]). Ignorance on the importance of defining the best possible test duration, misinterpreting of flow regimes and not detecting hydrates or scale deposition in the flow line are just a few examples where it can go wrong. Therefore, it is of major importance that the flow rate data is properly validated before it is stalled into an allocation database for further applications. With such a validation check we should get answers to the following question:

> *"Can we make sense of the data and is it applicable on the long term and viable for further applications?"*

At this moment, no uniform and unique procedure for flow rate measurement validation during a production test is available. There are existing methods but information is scattered and such methods are mainly focus on specific applications, problems and/or field cases. Hence, it is necessary that a comprehensive

overview on existing validation method is done. Before validation methods could be selected, combined in a procedure or workflow and applied to a specific device.

Finally, it is essential that proposed validation checks can be used in an automated fashion, because the average amount of production wells assigned engineer is currently around 300. This will only continue to grow in the future to around 800 in 2020, according to Liddell *et al.* [7].

PROBLEM STATEMENT

Dual gamma ray multiphase flow meters give a lot of information. Much more compared to data obtained with single phase flow meters on test separators, which has been the standard for the last few decades. However, the data from such a multiphase flow meter is still approached and analyzed in the same as test separator data, despite of all the extra information. The goal of this work is to define validation methods uniquely designed for dual gamma ray multiphase flow meter data. To validate flow rate measurements with data provided by the meter itself. This report will focus on the Vx meter, which is a dual gamma ray multiphase flow meter. In the case the reader is unfamiliar with this type of flow meter, appendix A will give a technical summary.

OBJECTIVES

The objective of this project is to define a series of potential validation criteria for production tests, using high-frequency and high-resolution data acquired from the Vx flow meters. The project will start from a comprehensive literature review in order to get an overview of all the existing production test validation and rate estimation methods. Also to identify which of those techniques could be applicable to high frequency Vx data. The most suitable technique, an adjusted choke model, then will be tested on actual flow metering results that will be provided. The analysis algorithms should be devised to determine which of the validation methods identified could be implemented in an automated fashion on Vx meter data. This also includes a way to properly identify representative flow data and to estimate optimal test duration.

OUTLINE

In chapter 2 a summary is given of the public literature review, it describes all known validation methods which can be applied on flow rate measurements. Furthermore, next to the public literature review an internal inquiry has been done in order to define existing flow rate validation issues with the Vx meter. The combination of the 2 reviews led to different leads. The first of them was a specific choke model which can be used to validate the flow rate of the Vx meter, which is described in chapter 3. Also, there was a lead to use signal analysis in order to define an ultimate production test duration with Vx meter data, this is explained in chapter 4. Finally, all the conclusions and recommendations are set out in final chapter 5.

2

LITERATURE REVIEW

The literature review consists of two parts. In the first part, as many as possible flow rate validation methods are defined out of public literature and categorized, in order to get a complete overview of existing methods. The second part consists of an internal inquiry in order to define existing issues with Vx multiphase flow meters, only experts working with the Vx meter were invited to participate. The goal is to connect validation methods with issues to define applications to solve them automatically.

2.1. PUBLIC LITERATURE REVIEW

Validation is a widely used term in literature for several definitions, even merely applied to flow rate measurement the keyword brings up a broad spectrum of results. Most papers only emphasize the importance and necessity of the validation of flow rate measurements but rarely go into detail on the methods itself. Therefore, a relevant definition of validation should be used. This brings up the following question which needs to be answered:

> "Can we make sense of the data and is it applicable on the long term and viable for further applications?"

With the help of this question, validation methods were defined. Those methods can be categorized in three groups:

1. Validation methods which check the meter performance
2. Validation methods where flow rate output of meter is compared with flow rates from reference devices or analytically calculated flow rates.
3. Validation of flow rate data by analysis of production trends.

VALIDATION BY CHECKING THE METER PERFORMANCE

Group 1 concentrates on methods which concentrate on the parts and the sensors of the meter itself. One of the most known methods is the empty pipe measurement a.k.a. baseline monitoring to validate meter sensors(Corneliussen *et al.* [2], Falcone *et al.* [8], Theuveny *et al.* [9]). A known fluid with known composition (or an empty pipe) is measured and compared to older tests. The measurement points should stay constant within a set tolerance band. This method is a standard validation method. Most multiphase flow meters need additional user input such as fluid properties (Jayawardane and Theuveny [10], Hollaender *et al.* [11]). Useful methods to validate such input parameters are for example an additional black oil model (BOM), equation of the state or periodic inline sampling. A very simple check that often is forgotten is keeping the production envelope in mind. Every meter is designed to work properly in a certain range of flow rates, temperatures, pressures, etc. It is also important to validate the condition of meter parts itself now and then. For instance, a meter could give erroneous measurements when the inside is plugged with; hydrates, scales or other participated solids. It is not always possible to quit production and check the inside of the meter. Therefor several methods exist to validate whether a meter is plugged or not during production (Shumakov *et al.* [12], Theuveny *et al.* [13]). Also, methods exist to validate the condition of measurement data in a more sophisticated way, with a self-diagnostic sensor chip (Henry [14], Henry *et al.* [15]. This chip is installed on a meter and uses several secondary parameters in order to define whether a measurement is faulty or not.

VALIDATION OF FLOW RATE MEASUREMENTS BY COMPARING FLOW RATES WITH REFERENCE DEVICES OR ANALYTICALLY OBTAINED FLOW RATES

By far the most validation methods described in literature can be related to group 2; simple comparison of measurement data with secondary obtained measurement data. In the most simple case it would be a comparison of measurement data with a reference meter. This can be single phase flow meters behind a test separator (Al-Saqabi *et al.* [16], Lomukhin *et al.* [17], Al-Khamis *et al.* [18]). Also, comparison with a master flow meter (fiscal allocation) at the end of the production installations is a used method. In this case the master meter will measure one well at the time and those measurements can be compared with the meter installed on the well (Corneliussen *et al.* [2]). This is called reconciliation factor (Corneliussen *et al.* [2]).

Furthermore, flow rate data can in theory also be modeled. Such a model is known as a virtual flow meter (VFM) in literature. The outcome of a VFM can be compared with actual flow rate measurements and obscure behavior in measurements can be detected. Several kind of VFM's are described in literature. One of them is the data validation and reconcilition (DVR) model. Here the whole production system is modeled with the help of mass balances and the average error of all the system components should be as small as possible (Couput *et al.* [19, 20], Haouche *et al.* [21], Petukhov *et al.* [22]).

Another VFM is based on down-hole pressure and temperature data. With the help of a Bayesian inversion methods, data from a permanent downhole gauge (PDG) can be translated to flow rates at the surface Duru and Horne [23]. Other more simple method which also uses PDG is by modeling the complete well bore and use the PDG and/or ESP sensors to model the flow rates at surface conditions (Al-Amri *et al.* [24], Caicedo and Montoya [25]). A VFM can also be based on choke data. An unconventional method uses acoustic noise over the choke and estimates flow rates of different fluid phases (Piantanida *et al.* [26]). The most important conventional method uses the pressure drop (bernoulli's equation) over the choke in order to predict the mass flow rate (Falcone *et al.* [8]).

A VFM can also be described as a 'white box model' as it uses actual physical relationships. Flow rates can also be modeled with 'black box modeling'. With the help of a neural network (NN) for example (Falcone *et al.* [8], Lindsay *et al.* [27]). A NN can be trained with actual measurement data sets from a certain meter. When the NN is trained it can predict flow rates which can be compared with the actual flow rate measurements from a meter.

Finally, a meter can also be validated by comparison with another measurement technology. For instance with tracers (Corneliussen *et al.* [2]). Upstream of the meter a tracer is injected and downstream samples are taken where the dilution of the tracer is measured which can be translated to a flow rate estimation.

VALIDATION OF FLOW RATE DATA BY ANALYSIS OF PRODUCTION TRENDS

The final group of validation methods consists of validation of the data itself, assuming a perfectly working meter. Because data can still be faulty when a meter is used in a wrong way. In the case of a production test which could not reach a steady state for example.

The most basic way to check the usefulness of flow rate data is by quality check with history data. The flow rates can be compared to a prediction based on history data and expected production (Quevedo *et al.* [28]). One could also think of the comparison between different production ratios. Such as the gas oil ratio (GOR) and gas liquid ratio (GLR) for example, in combination with a check if they make sense. Diagnostic plots can also help in analyzing the measured flow rates. Any inconsistency in a production test can be shown by just plotting them.

Finally, in literature on chemical reactor technology several methods are described which use signal/noise analysis in order to validate flow rate production test data (van der Hagen [29]).

2.2. SCHLUMBERGER EXPERT ENQUIRY

Subsequently to the literature review an inhouse inquiry[1] has been held in order to define as much Vx meter issues as possible which can occur during a production test. These are the issues we want to detect with the validation methods.

ISSUES ASSOCIATED WITH FLOW CONDITIONS

Issue: Change in water property In Vx technology the density of the phase is user input. Density can be defined by sampling, lab, inline automatic sampling with the PhaseSampler, or with the aid of a black oil model (BOM). According to the experts it happens that the water density input is wrong. A reason for that

[1] Within carefully selected Schlumberger employees on expertism or extensive operational experience with Vx meters.

could be a change in the salinity of the water during a production test. When the density is of this will have an influence on the flow rate calculations. The problem can be detected by: observing coherent changes in the WLR and GOR or by taking manual water property measurements. The current solution to this issue is to take new samples and update water densities and mass attenuation.

Issue: Inappropriate Test Sequence It can happen that stable flow conditions are earlier reached than noticed during a test, so the test could have been concluded earlier. Or that no stable conditions is reached over the whole test, then the test should be declared unstable and be redone. An automated detection method is not existing yet and in this study, see chapter 4, an automated algorithm is proposed to answer this issue.

Issue: Meter outside of operation envelope It can happen that the meter works outside of its intended production envelope. Observing a very high or low DPV could be a way to detect this.

Issue: Change in HC properties The produced fluid properties can change over a production test. This can be detected by observing a change in the GOR while the WCT is constant.

TECHNICAL ISSUES IN THE METER DURING OPERATIONS

The issues in this groups mainly concentrate on broken parts of the meter such as sensors.

Issue: Water in the Source compartment It can happen that the compartment which holds the Barium-133 source of the meter is not water resistant anymore and filled with water. This influences the nuclear gamma ray counts at the detector and therefor gives erroneous fractions. The following behavior can use as possible detection method. It shows as an increase in the liquid fraction over time (not continuous but random with a downward trend) and a change in water cut.

Issue: Sensor drift A broken sensor can result a drifting sensor. This can be detected by comparison with other sensors. A pressure sensor drift can be detected for example by comparison between the pressure sensor and the GOR trend. Also the choke model, proposed in chapter 3, can be used to detect sensor deviation over time. For example a DPV sensor drift.

ISSUES ASSOCIATED WITH INPUT PARAMETERS

The Vx meter models need user input in order to make all kinds of calculations, see appendix A. It can happen that wrong user input influences the calculated flow rates.

Issue: Wrong oil type selected in the model In case the wrong oil type is selected the meter will give a huge under or overestimation of the gas flow rate, this could be detected with a choke model as described in chapter 3.

Issue: Wrong density conversion The BOM can calculate the wrong local densities. Due to a poor mass balance for example. This can be detected taking fluid samples locally and analyze them in a lab. Also another BOM could be used to back check the density conversion.

Issue: Wrong in-situ or PVT input An in-situ is running a 100% oil, water (brine) or gas in order to define the Vx meter nuclear solution triangle, see figureA.3. Sometimes a wrong in-situ can influence the meter results. This can be detected by observing the difference in mass attenuation between different wells which produce the same reservoir, they should not vary a lot. Another method of detection is observing that the operating point moves out of the nuclear solution triangle. Solution is to re-do samples or re-do an empty pipe measurement check to obtain updated in-situ's.

Issue: Wrong viscosity user input It can happen for whatever reason that the oil viscosity input in the model is wrong. This can be detected when software processes very large flow rates. It might be detected by observing the temperature and GOR behavior, in the case both parameters go up there might be something wrong with the viscosity or BOM.

Issue: Wrong CNF file A Vx meter uses a configuration file (CNF) to recognize a specific production well to use the right model inputs. However, it could happen that the wrong CNF is used for a well. The Vx meter will produce erroneous values. The only known detection method is by comparisson with client results.

2.3. CONCLUSION LITERATURE REVIEW

A comprehensive public literature review has been done in order to define an overview of existing flow rate validation methods. The methods are accordingly categorized into an appropriate grouping. Such an overview was not existent yet in public literature. Subsequently, an internal inquiry with selected Vx meter experts has been done with a focus on current issues with Vx meters. This overview of issues is based on the participation of 11 experts with extensive experience with Vx meters in field operations or research. The final step was to connect available validation techniques with actual Vx meter issues in order to design automatic detection methods, to flag such issues, which was the initial goal of this work.

In chapter 3 a new choke model is proposed to run in series with a Vx meter, in order to: detect a drift in the DPV sensor output of the VX; detect the under- or overestimation of the gas flow rate calculated by the Vx model or to detect whether the Vx meter is working in the intended operation envelope or not.

The issue of the inappropriate test sequence is solved in chapter 4. A method is proposed which automatically defines whether a production test is stable and can be concluded or rejected.

Not all of the Vx meter issues coming from the inquiry could be resolved with automated validation methods due to the limited available time. However, they are still included in this chapter as a lead for future work.

3

APPLICATION OF A THEORETICAL MULTI-PHASE CHOKE MODEL FOR FLOW MEASUREMENT VALIDATION

The literature review concluded that a choke model could be a proper validation method applicable for validating flow rate measurements from a Vx meter. A choke model is a physical model for the flow through a restriction.

Choke models are already used sporadically to validate flow rate measurements of the Vx meter. However, in those cases mainly empirical defined choke models are used. Those models can only account for critical flow or sub-critical flow separately. Also, theoretical defined choke models based on a material balance exist. These kind of models can account for both sub-critical and critical flow. However, these models do not account for the slippage of gas which is an important factor in a multiphase flow and therefore no model is ideal.

An investigation in recent literature pointed out a recently added choke model. This model is adjusted, applied and tested on Vx meter data in this study. This model should work in all cases and be a standard validation method to validate flow rate measurements.

The model is able to define the critical/sub-critical flow boundary and is capable of defining the mass flow rate for critical and sub-critical flow. The model includes the slippage of gas and is therefore more accurate than older currently used choke models.

This chapter will first discuss choke models for two-phase (gas-liquid) flow in general. Then a compact overview of existing choke models is given. In section 3.3 the proposed choke model for Vx meter flow rate validation is explained. This model is mathematically derived in appendix B. In section 3.4 the error propagation of the model is discussed. The model is programmed into Matlab and Excel VBA.

3.1. CHOKE RESTRICTION

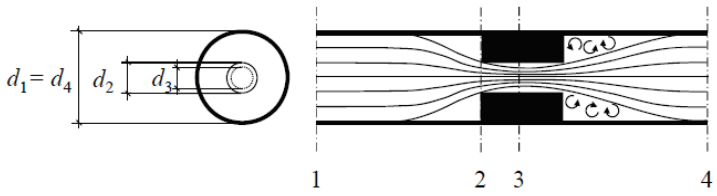

Figure 3.1: Schematic cross section of a choke restriction geometry, Jansen [30].

Chokes are common restrictions encountered in a production system occurring just after the production tree, see figure 3.1. The main goals of a choke are: to restrict the flow rate if necessary; to reduce the pressure downstream of the choke and to decouple the upstream process from downstream influences. However, the pressure difference over a choke can have a secondary usage, it can also give a prediction about the flow

rate. The flow through a choke can be separated into 2 parts. A converging part (between point 1 and 3) and a diverging part (between point 3 and 4). The differential pressure over the converging part can be modeled relatively easy with the Bernoulli equation and the right assumptions. The diverging part holds more complex behavior. In this region, downstream of the restriction, strong turbulent flow occurs which includes large vortices or areas of flow reversal. The turbulent flow results in dissipation of energy and a permanent reduction in pressure between the upstream and the downstream pressure of the restriction. This permanent pressure reduction is very difficult to model as complex thermodynamical behavior is involved.

Flow behavior There are two types of flow behavior through restrictions: Critical and sub-critical flow. Critical flow occurs when the speed of the flow through the throat (smallest section) reaches Mach 1, also called sonic flow, which means that the velocity of the flow is the same as the velocity of sound. When the velocity is smaller than the velocity of sound it is called sub-critical flow. In sub-critical flow the flow rate is related to the pressure drop across the restriction. Pressure fluctuations downstream are able to propagate through the restriction. In critical flow the flow rate is only related to the upstream pressure. Therefore, reduction of the downstream pressure does not affect the upstream pressure as the reduction of pressure cannot be transmitted through the restriction. When the velocity is higher than the velocity of sound, it is called super-critical flow, which is rarely encountered in production systems and disregarded in this report.

Sub-critical/critical flow boundary Choke models have generally been used and researched as an extra production control method, because it is very important in production to operate with critical flow conditions. Then the downstream effects cannot propagate backwards through the choke and damage the reservoir section. Hence, a good approximation of the sub-critical and critical boundary of the flow have always been very important.

3.2. EXISTING CHOKE MODELS

Existing models for two-phase flow (gas & liquid) are either empirical or theoretical.

3.2.1. EMPIRICALLY DERIVED MODELS

Models such as Gilbert [31], Ros [32], Achong [33], Pilehvari [34], Ashford and Pierce [35], Osman and Dokla [36], Omana *et al.* [37] are empirical choke models, with coefficients obtained through curve fitting of a large set of experimental data. These models are all developed for specific fluid properties and pressure and flow rate ranges, and these models cannot be used beyond those ranges. Furthermore, most empirical models do not account for sub-critical flow behavior and are only applicable in critical flow conditions.

3.2.2. THEORETICALLY DERIVED MODELS

Next to the empirical models, there are also theoretically derived models. The theoretical approach means that the models are derived from mass, momentum and energy balances. Published examples are Al-Safran and Kelkar [38], Perkins [39], Sachdeva *et al.* [40], Schüller *et al.* [41]. Theoretical models have the ability to be used in a much wider range of fluid properties and operating conditions than empirical models. Therefore, they are the most popular kind of choke model in the industry.

Sachdeva et al. (1986) This model is derived from 1D balance equations for mass, momentum and energy of two-phase mixture of gas and liquid, based on the following assumptions:

- 1D flow;
- Phase velocities are equal at the throat (homogeneous mixture), so no slip assumed;
- The predominant pressure term is acceleration;
- The gas quality (flowing gas mass fraction) is constant;
- The liquid phase is incompressible;
- The gas expands polytropical;
- Flow is adiabatic and frictionless.

The resulting equations are capable of finding the boundary between sub-critical and critical flow, and to calculate pressure drop for given flow rates and fluid properties in both the critical and the sub-critical regime (Sachdeva *et al.* [40]).

Perkins (1993) This model is derived from 1D balance equations for mass and energy. Contrary to, Sachdeva *et al.* [40], the model uses the gas-phase energy equation instead of the mixture momentum equation (Perkins [39]).

Selmer-Olsen(1995) This model uses a "control volume" approach. The model is derived from the local cross-sectional averaged balance equations of mass, momentum and energy for steady-state flow of a multiphase mixture. The control volume approach features a more mechanistic description of the irreversible-loss process than a discharge coefficient only, such as in the Perkins and Sachdeva models. The slip ratio is included in the model and the model can account for the slippage of gas. However, the control volume approach which is more accurate results in a complex formulation which makes it less ideal (Schüller *et al.* [41]).

Al-Safran (2009) Developed on the basis of the Sachdeva and Perkins models. The model is derived from 1D balance equations of Mass, Momentum and Energy for two-phase flow across a restriction. Also, a slip ratio model is applied so the model can account for slippage of gas through the liquid as well. The slip model is capable of calculating the critical/sub-critical flow boundary and mass flow rate. The model can be reduced to Perkins or Sachdeva when assumptions are simplified (Al-Safran and Kelkar [38]).

Jansen (2014) The model is derived from 1D Mass and Momentum balances for two phase flow across a restriction. The polytropic bernouli equation is derived from these balances. The model gives a relation between the temperature drop and pressure drop over the converging part of the choke. This model is essentially the same as the Al-Safran model without slippage of gas. The same inverse density and velocity terms for no-slip as in Sachdeva *et al.* [40] are used. This model is capable of calculating the pressure difference of a restriction when flow rates are known (Jansen [30]).

Assumptions	Sachdeva	Perkins	"hydromodel"	Al-Safran	Jansen
Material balance	Mass, momentum & energy	Mass & energy	Mass, momentum & energy	Mass, momentum & energy	Mass & Momentum
1D flow	V	V	No	V	V
Predominant pressure term is acceleration	V	V	V	V	V
GOR remains constant "frozen flow"	V	V	V	V	V
Liquid phase incompressible	V	V	V	V	V
Flow is adiabatic and frictionless	V	V	V	V	V
Gas expands polytropical	-	V	V	V	V
Slippage of gas is accounted for.	-	-	V	V	-

Table 3.1: Overview of assumptions in theoretical choke models

3.3. PROPOSED CHOKE MODEL

In this chapter the implemented choke model is explained, it will predict a mixture multiphase mass flow rate through the restriction based on differential pressure and a known mass fraction x_g of gas. In the case the mixture density ρ_m is known, the multiphase mixture volumetric flow rate q_m can be calculated. The model is mainly based on Jansen [30] however derived in a way such that slippage of gas is included. Which is similar with the approach used in Al-Safran and Kelkar [38]. In Appendix B all of the expressions used in this chapter are derived.

3.3.1. MODEL EXPRESSIONS

Relation downstream pressure to throat pressure Only the differential pressure behavior on the convergence part of the choke (between point 1 and 3) can be modeled. In order to do so the downstream pressure p_4 needs to be related to the throat pressure p_3 in some way.
In the case of sub-critical flow conditionns Perry's relationship can be used:

$$p_3 = p_1 - \left(\frac{p_1 - p_4}{1 - \left(\frac{d_3}{d_4}\right)^{1.85}} \right) \tag{3.1}$$

This relationship, also proposed in Al-Safran and Kelkar [38] and Perkins [39], makes a guess for the throat pressure (p_3) using pressure measurements up- and downstream (p_1 & p_4) of the choke. d_3 is the throat diameter and d_4 is the downstream pipe diameter.

Critical-flow boundary Before the mixture mass flow rate can be calculated the current flow conditions should be known. This is found by the use of an implicit equation to define the critical pressure ratio. The following expression as derived in Appendix B.3.1 is used:

$$p_{r,crit}^{\frac{n-1}{n}} = \frac{\alpha\left(1 - p_{r,crit}\right) + \frac{n}{n-1}}{\frac{n}{n-1} + \frac{n}{2}\left(1 + \alpha p_{r,crit}^{\frac{1}{n}}\right)^2} \tag{3.2}$$

Where $\alpha = \frac{R x_l \rho_{g,1}}{x_g \rho_l}$ to simplify the expression and n the polytropic heat coefficient, as explained in Appendix B.2:

$$n = 1 + \frac{x_g(c_{pg} - c_{vg})}{x_g c_{vl} + (x_g - 1)c_{vl}} \tag{3.3}$$

$p_{r,crit}$ is the pressure ratio $p_r = \frac{p_3}{p_1}$ when critical flow behavior occurs. x_g is the gas quality (flowing gas mass fraction), and x_l is the flowing liquid mass fraction, $x_l = \left(1 - x_g\right)$. c_{pg} & c_{vg} are specific heat capacities of gas at constant pressure and volume respectively, c_{vl} is the specific heat capacity of liquid at constant volume, this is further explained in appendix B.2. $\rho_{g,1}$ is the density of the gas at the inlet of the choke restriction and R is the slip ratio which is the ratio between the liquid and gas velocity, $R = \frac{v_g}{v_l}$. Because the gas and liquid velocities are unknown it is required to use slip ratio models, which are defined in equation 3.6 & 3.7.

Critical and sub critical mass flow rate The complete derivation is given in Appendix B.3.2. The final form to calculate the mass flow rate, $\dot{m}$, is as follows:

$$\dot{m} = C_d A_3 \sqrt{\frac{2\rho_{g,1} p_1 \left[\frac{n}{n-1}\left(1 - p_r^{\frac{n-1}{n}}\right) + \alpha\left(1 - p_r\right)\right]}{x_g \left[p_r^{-\frac{1}{n}} + \alpha\right]^2 \left[x_g + \frac{x_l}{R}\right]}} \tag{3.4}$$

The expression for the pressure ratio p_r is depending on whether the flow is sub-critical or critical. In the case of $p_r < p_{r,crit}$ critical flow conditions are assumed and $p_r = p_{r,crit}$ is valid, equation 3.2. Otherwise, when $p_r > p_{r,crit}$ a sub-critical flow is assumed and the pressure ratio $p_r = \frac{p_3}{p_1}$ should be used, p_3 is assumed with Perry's relationship, equation 3.1. The discharge coefficient C_d is a very important factor which pragmatically

accounts for the irreversible losses over the choke. The discharge coefficient can also adjust for unknown phenomena in the choke, so C_d also serves as tuning factor. A_3 is the cross sectional area of the throat.

Slip ratio for sub-critical flow In Schüller *et al.* [41] a comprehensive study was performed on the slip ratio R. Several slip-ratio models where tested in order to find the best slip-ratio per case. The Grolmes and Coates [42] slip ratio model in equation 3.5 was founded to be most accurate for sub-critical flow behavior.

$$R = a_0 \left(\frac{1 - x_g}{x_g} \right)^{(a_1 - 1)} \left(\frac{\rho_l}{\rho_g} \right)^{(a_2 + 1)} \left(\frac{\mu_l}{\mu_g} \right)^{a_3} \tag{3.5}$$

In Al-Safran and Kelkar [38] it is recommended to use for the slip-ratio model the model constants; $a_0 = 1$, $a_1 = 1$, $a_2 = \frac{-5}{6}$ and $a_3 = 0$. These constants originate from Simpson *et al.* [43]. Implementing these model constants in 3.5 the slip ratio for sub-critical flow becomes a ratio between the liquid and gas density:

$$R = \left(\frac{\rho_l}{\rho_g} \right)^{\frac{1}{6}} \tag{3.6}$$

Slip ratio for critical flow In the case of critical flow together with the assumption of gas slippage through the choke, the same formula for inverse mixture density $\frac{1}{\rho_m}$ can be used, equation B.10. However, for R, the Schüller *et al.* [44] slip-ratio for critical flow should be used, which is recommended by Al-Safran and Kelkar [38].

$$R = \sqrt{1 + x_g \left(\frac{\rho_l}{\rho_g} - 1 \right)} \left(1 + 0.6 e^{-5.0 x_g} \right) \tag{3.7}$$

3.3.2. MODEL CODING

Computational logic The computational logic is shown in figure 3.2. The first step is to guess p_3 with 3.1. Then, the pressure ratio p_r can be calculated by iteration, by solving 3.2 for $p_{r,crit}$.

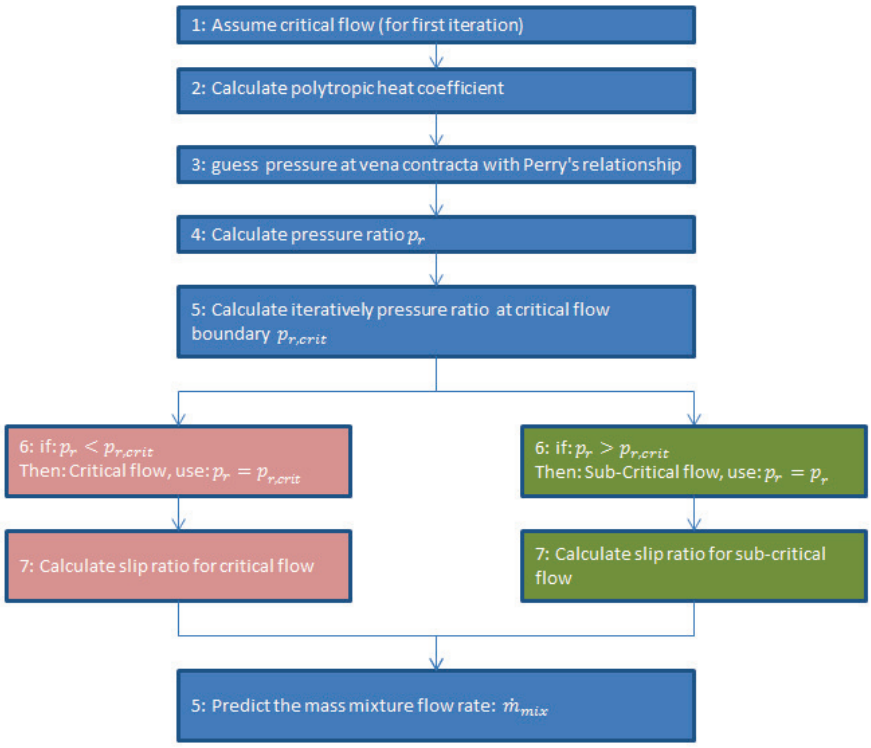

Figure 3.2: The flow diagram shows the sequence of calculations of the model

In the case $p_{r,crit} < p_r$; critical flow is assumed and $p_{r,crit}$ should be used for p_r in equation3.4 to calculate the mass flow rate. For the slip-ratio R equation 3.7 is chosen. In the case $p_{r,crit} > p_r$; sub-critical flow is assumed and the pressure ratio p_r can be used in equation 3.4 to obtain the mass flow rate. Equation 3.6 is necessary for the slip ratio R. Finally, the discharge coefficient (or "tuning factor") C_d of the choke needs to be defined and tuned against actual reference data before the model works accurately. This is done by least squares assuming an Gaussian Error distribution in the data.

The choke model is coded both into Matlab and Excel VBA following the logic in figure 3.2 in order to test the model on data.

3.4. RESULTS AND DISCUSSION.

This section gives the results on a field validations, performed on actual Vx flow meter data sets.

Set-up In order to perform a good flow rate validation on the Vx flow meter the choke model should be used in series with the meter; the meter should always be calibrated before the choke model can be used. After start of a production test the choke model has to be tuned for a certain amount of time to define the right discharge coefficient C_d.

The Vx meter can be located upstream or downstream with respect to the choke. This is represented in figure 3.3 & 3.4. Set-up 1 represents the Vx meter deployed upstream of the choke. This is an ideal set-up for the choke model because the already known fluid property input used in the Vx meter can also be used for the choke model. Unfortunately, this set-up is used rarely due to possible hydrate formation in the Vx meter. The Vx meter is generally deployed downstream of the choke, which is shown in figure 3.4. In this case the fluid properties, the gas and liquid density ρ_g & ρ_l, need to be converted to the right local conditions at the inlet of the choke, as there is no information. This introduces an extra error, depending on the black oil model (BOM) used for the transformation.

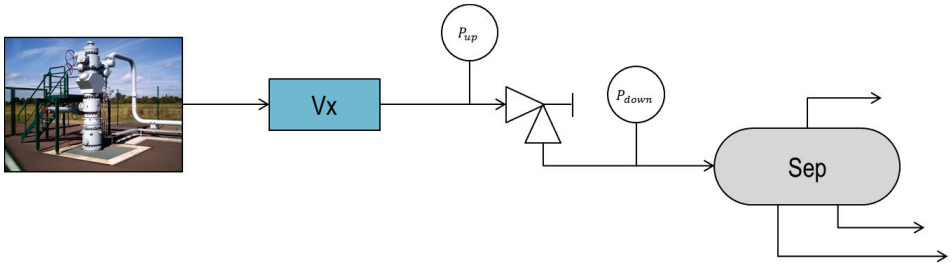

Figure 3.3: Setup 1: Vx deployed upstream of the choke

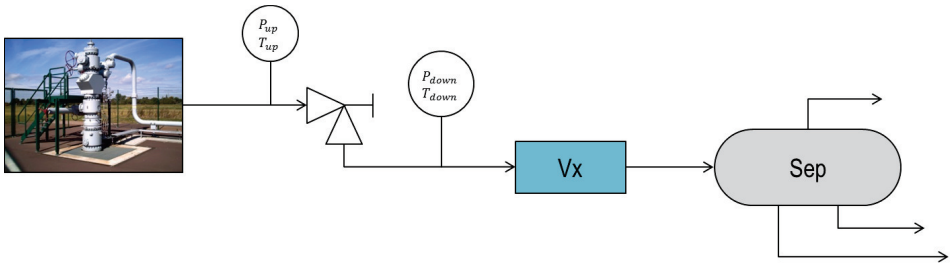

Figure 3.4: Setup 2: Vx deployed downstream of the choke

Data sets To test the choke model, presented in section 3.3, various data sets have been used. Initially, constant production data from gas and oil wells. Subsequently, data sets with more difficult fluids to predict were tested, such as waxy or heavy oil wells.

VX METER UPSTREAM OF THE CHOKE

The first field validation study is carried out to test the choke model on actual Vx measurement data. Firstly, the choke model is tested on set-up 1, as shown in figure 3.3, because it is important to exclude as many external factors as possible. In this case the BOM is such an external factor which is not needed in set-up 1.

The available data for the field validation study, with the Vx meter upstream of the choke, consists of 96 data points. Those data points originate from 5 different production tests. The data points represent averages of constant periods of flow. A data point consists of all the Vx meter output plus, manually taken, pressure and temperature measurements up- and downstream of the choke. The choke model uses this manual measured differential pressure over the choke to predict the mixture mass flow rate. One third of the data points is used to tune the discharge coefficient C_d for all the 5 cases. The prediction is compared with the measured values from the Vx meter, as can be seen on figure 3.5. This figure represents the accuracy of the choke model on

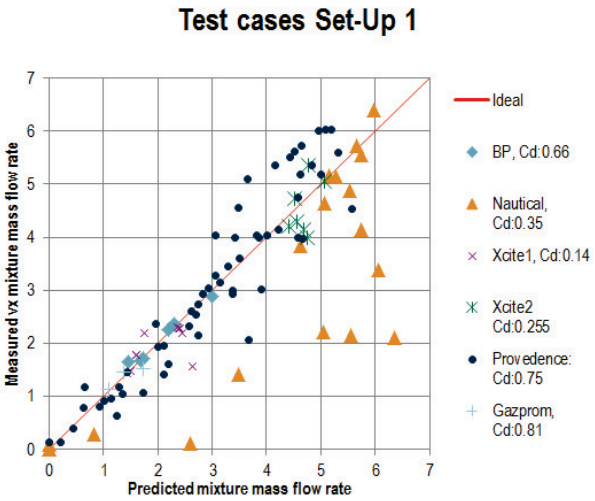

Type choke:	Case:	Type well:
Fixed choke *(9 data points)*	BP	Heavy oil
	Gazprom	Gas well
Adjustable choke *(87 data points)*	Nautical	Heavy oil
	Xcite	Very Heavy oil
	Providence	Waxy oil

Figure 3.5: Prediction vs. measured mass-flowrate (96 datapoints originated from 5 different production environments).

each field test. The results show clearly that some cases are pretty accurate, such as the BP and Gazprom case, while others are more off, such as the Nautical, Xcite and Provicence cases.

Initially, it was thought that this difference in accuracy was due to the fluid properties. However, this is not the case. The BP case, which is a heavy oil, is fairly accurate with respect to the Providence data which consists of waxy oil.

An important parameter to analyze the choke model performance is with the discharge coefficient C_d, or tuning factor. This factor should be somewhere between 0.6 and 0.9 in order to represent irreversible pressure losses over the diverging part of the choke. However, some of the cases have a very low C_d, such as the Nautical and Xcite cases. These cases consists of heavy to very heavy oils, which introduces extra friction over the choke. This is an indication that the choke model is less useful at wells with very heavy oil.

Parameter sensitivity study Even in an ideal field case there is always some error observed in field cases, such error can be attributed to the noise and scatter existing in field data. However, a model can be more sensitive to one input parameter compared to another. Therefore, a sensitivity study has been performed on the model. The study is done on critical and sub-critical flow data, as the model works slightly difference depending on the conditions present in the choke. Figure 3.6 shows a tornado plots which represents how the output of the model is influenced by altering the input parameters from -10% to 10%.

d_c stands for the choke diameter of the choke. The overall discharge coefficient or tuning factor C_d is established with the help of least squares method. P_{up} and P_{down} are respectively the pressure up- and downstream of the choke. $\dot{m}_g$ and $\dot{m}_m$ are the gas and mixture mass flow rate and output of the Vx meter, these parameters are used to calculate the gas quality x_g. d_1 is the diameter of the pipe at inlet of the choke. For some input parameters such as the pressure, it is highly unlikely that the uncertainty is 10% percent. However, in the case of the choke diameter of an adjustable choke it is very common that such an uncertainty exists.

The results of the sensitivity study in figure 3.6 reveal that the choke model's most sensitive parameter is the choke diameter. This can give an explanation why some of the predictions are far off, because an adjustable choke with high uncertainty in the choke diameter will have a larger error then a prediction on a fixed choke. Therefore, the same data as in figure 3.5 has been plotted in figure 3.7 with a distinction between adjustable and fixed choke data.

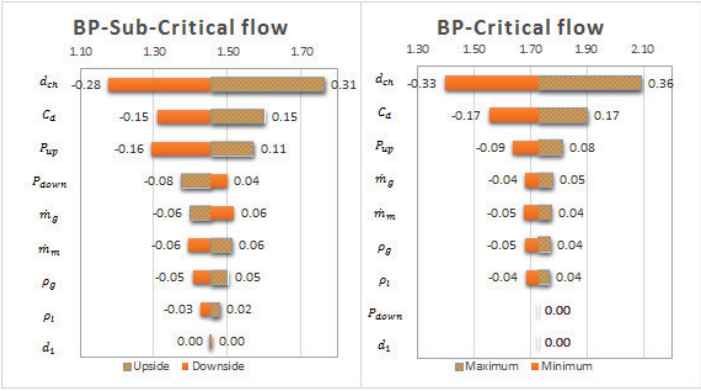

Figure 3.6: Sensitivity study of the choke model on sub-critical and critical flow data.

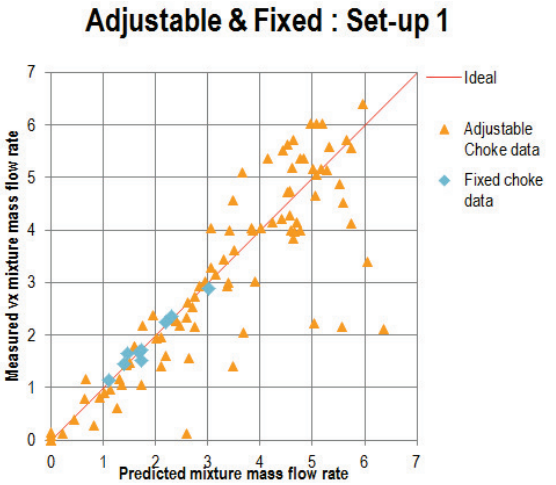

Cases: Set-up 1		e_1	e_2	σ
Fixed choke	*9 data points*			
BP	Heavy oil	-1.67%	3.50%	4.06%
Gazprom	Gas	1.64%	7.02%	5.23%
All fixed choke data		-0.56%	4.67%	4.50%
Adjustable choke	*87 data points*			
Xcite	Heavy oil	4.99%	11.65%	15.88%
Nautical	Very Heavy oil	17.62%	24.70%	50.06%
Providence	Waxy oil	5.70%	18.58%	20.69%
All adjustable choke data		7.36%	18.13%	31.16%

Figure 3.7: Prediction vs. measured mass-flowrate as in figure 3.5 with a distinction between fixed and adjustable choke data

Clearly, figure 3.7, underlines the statement of the choke model being more accurate with a fixed choke. A statistical error analysis on the data point shows the difference even better.

statistical error analysis On all the data points a statistical error analysis has been performed in order to define how the choke model is performing on the different cases, by calculating the average percent error (e_1), the absolute average percent error e_2) and the standard deviation (σ):

$$e_1 = \left(\frac{1}{n} \sum \frac{\dot{m}_{predicted} - \dot{m}_{Vx}}{\dot{m}_{Vx}} \right) \times 100\% \tag{3.8}$$

$$e_2 = \left(\frac{1}{n} \sum \left| \frac{\dot{m}_{predicted} - \dot{m}_{Vx}}{\dot{m}_{Vx}} \right| \right) \times 100\% \tag{3.9}$$

$$\sigma = \sum_{i=1}^{n} \sqrt{\frac{\left(\left| \frac{\dot{m}_{predicted} - \dot{m}_{Vx}}{\dot{m}_{Vx}} \right| - e_1 \right)^2}{n-1}} \tag{3.10}$$

In the calculated results in the table on the right in figure 3.7, it can be seen that the fixed choke data gives very satisfactory results. The adjustable choke data accuracy on the other hand gives differs per case. This is due to the high uncertainty of an adjustable choke.

3.5. CONCLUSION

In this chapter a choke model has been proposed to validate flow rate measurements from a Vx multiphase flow meter and tested on actual data.

- The choke model is able to predict the flow rate with a satisfactory accuracy in the case of a fixed choke. An adjustable choke has a very high uncertainty and this has a considerable influence on the prediction accuracy. Therefore, the model should preferably only be used on fixed choke data and conclusions based on results with an adjustable choke should be taken with caution.
- Slippage phenomenon between the gas and liquid phases in the choke exists and the model is able to correct for this.
- The model is able to recognize sub-critical and critical flow and corrects for this.
- The results shows that the model works on different fluid compositions. Waxy-, heavy oil wells and gas wells for instance.
- With respect to validation methods the choke model is able to:
  - Detect a drift of the DPV sensor output in the Vx meter.
  - Detect the under- or overestimation of the gas flow rate calculated by the Vx model.
  - Detect whether the meter is operating in the operation envelope or not.
- For any choke, the choke model needs an initial training period in order to tune the overall discharge coefficient C_d to the specific situation.
- The Vx meter has to be calibrated before it is used to tune the choke model. Once the overall discharge coefficient is tuned correctly it is able to detect Vx meter issues.

4

APPLICATION OF SIGNAL FLOW ANALYSIS FOR PRODUCTION TEST TIME OPTIMIZATION

In a production test, it is very important to have an optimized testing time as this makes it possible to reduce associated costs or increase test capacity. In order to be successful in a production test, a stable flow regime has to be established. From the moment stable flow is reached the test can be concluded. Therefore, it is essential to have proper techniques/methodologies available to define whether a stable flow has been established or not.

Currently, The most common way to decide whether the flow is stable or not is by simple ad-hoc methods varying per operator, such as observing the parameters obtained by measurements and their behavior over time compared against some stabilization criteria. An example criteria could be; the pressure should not deviate more then 1 bar per hour and the temperature not more than 1°C.

Such ad-hoc methods are, in principle, good methods to properly define a stable flow. Nonetheless, these methods only work for a constant flow regime. For instance, in the case of a slug flow regime such stabilization criteria will never be met. In those cases, the duration of a production test is defined on experience.

Now, with data from the Vx meter more parameters with higher frequency are available. This provides us with more and better information compared to measurements from a conventional test separator. Therefore, the obtained Vx meter data should not be treated the same as conventional data. This brings us to the following research question:

> *"Are there methodologies available to extract more information from Vx meter data in order to define an ultimate production test duration?"*

In this chapter several applications from the signal analysis domain are introduced, which can help in analyzing a production test to define an optimal test duration. Furthermore, several applications to do this are proposed in the form of automatic checks on the data and are ready for implementation.

4.1. MULTIPHASE FLOW REGIMES

This section gives a small introduction on multiphase flow behavior during a production test and its relation with the Vx meter.

Multiphase flows are very difficult to understand and predict. Common existing principles to define single phase flow characteristics are not applicable in this domain.

A multiphase flow can occur in a lot of different patterns. This is described in flow regimes, whose characteristics depend on certain parameters. Flow regimes are not under the control of the designer or operator, they vary depending on operating conditions, fluid properties, flow rates and the orientation and geometry of the pipes.

Transition between different flow regimes can be direct or gradual. Determination of the flow regimes during operation is very complex. However, in literature various experiments have been performed where

flow regimes are predicted. Usually, with the analysis of certain parameters such as pressure and temperature in combination with the observation of the flow in a transparent tube. This method is used to correlate flow regimes with the fluctuation behavior of specific parameters. The description of flow regimes depends mainly on the interpretation of the observer and is hence arbitrary in some degree.

4.1.1. THE MAIN MECHANISMS BEHIND THE FORMING OF FLOW REGIMES DURING OPERATIONS

The main mechanisms in forming a flow regime are transient-, geometry- and hydrodynamic effects or a combination of them. Corneliussen *et al.* [2]

- **Transient effects:** A transient effect occurs when the system's boundary conditions change. Such as the opening and closing of a valve.
- **Geometry effects:** Pipeline geometry or inclination have an enormous effect on the regime. This can be important for example in the flow between a subsea tieback and a production platform. Severe riser slugging is an example of this effect.
- **Hydrodynamic effects:** In the absence of transient- and geometry effects, the stable flow regime is entirely determined by flow rates, fluid properties, pipe diameter and inclination.

When hydrodynamic gas-liquid flow regimes are considered, the flow regimes can be grouped in dispersed flow, separated flow, intermittent flow or a combination of these.

- **Dispersed flow:** The flow regime is in both the radial and axial directions uniformly distributed. Examples of such flows are *bubble flow* and *mist flow* (Figure 4.2).
- **Separated flow:** The flow regime in the radial direction is non-uniformly distributed. However, the flow in the axial direction is uniformly distributed. Examples of such flows are *stratified flow* and *annular flow* (Figure 4.1).
- **Intermittent flow:** The flow regime is in both the radial and axial direction non-uniformly distributed. Examples of such flows are *elongated bubble flow* , *churn flow* and *slug flow* (Figure 4.2).

Flow regime effects caused by liquid-liquid interactions are insignificant compared to those caused by liquid-gas interactions. In this context, the liquid-liquid portion of the flow can often be considered as a dispersed flow.

HORIZONTAL FLOW REGIMES

In horizontal flows, the transitions are functions of factors such as pipe diameter, inter-facial tension and density of the phases. Figure 4.1 gives an overview of most of the horizontal flow regimes and how the transitions are dependent on superficial gas and liquid velocities. Such a map is only valid for a specific pipe, pressure and specific composition of the fluid. Hence, it is not useful in actual operations for flow regime detection, as most of the necessary parameters are not identical or similar to those used when building flow maps.

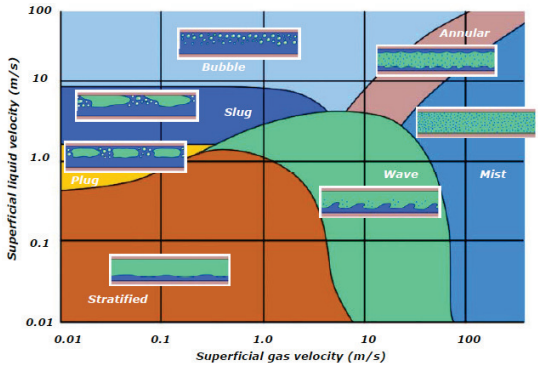

Figure 4.1: A generic two-phase horizontal flow map, Corneliussen *et al.* [2].

VERTICAL FLOW REGIMES

See figure 4.2 for an overview on most of the vertical flow patterns. An interesting observation in vertical flow is that the multiphase flow regimes can easily be described versus the increase of gas flow rate. If there is little gas, the flow will probably be a bubble flow. If there is an increase in the rate of the gas, bubbles will start to collapse in certain parts of the pipe and they will generate larger and faster bubbles called Taylor bubbles (slug flow). When the gas flow rate increases even more, a churn flow establishes and finally an annular flow regime will establish, where the liquid flows primarily as a film on the pipe wall with some en-trained liquid being dispersed in the gas core. When the gas volume fraction (GVF) surpasses 98%, mist flow (wet gas) is typically observed. Other dimensionless parameters, such as the Lockhart-Martinelli parameter can be used as limit conditions to predict annular mist flow. These are the flow patterns which are most likely to occur in the Vx meter during operation. Note that the borders between the regimes in figure 4.2 & 4.1 have to be interpreted as a transition area and not as a tight border.

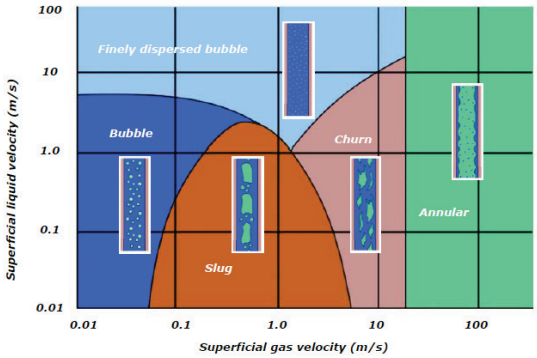

Figure 4.2: A generic two-phase vertical flow map, Corneliussen *et al.* [2].

4.1.2. MULTIPHASE FLOW BEHAVIOR IN THE VX METER

According to the previous section it is clear that multiphase phenomena in pipes are difficult to understand and predict. The flow regimes in a Vx meter are similarly complex. See figure 4.3 for a cross section of the Vx meter. In this cross section the complex behavior of multiphase flow is illustrated based on simulated conditions.

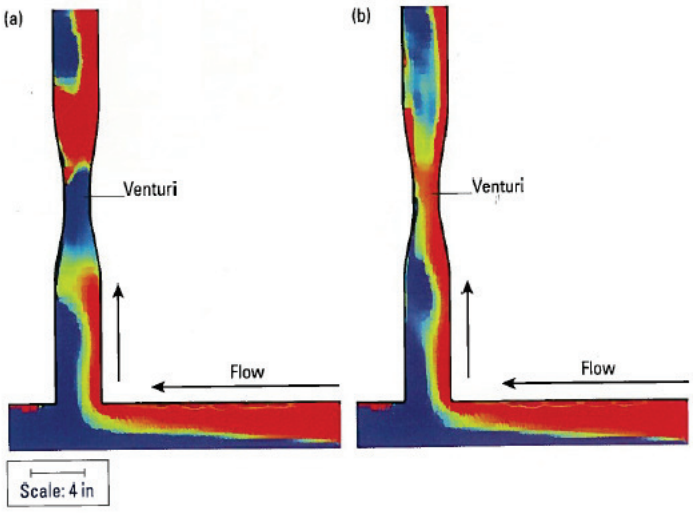

Figure 4.3: Simulation of flow in the presence of blind-tee and venturi configuration. (a) slug of water. (b) slug of gas. Pinguet [45].

The venturi section in the Vx meter is placed in a vertical configuration, so that the flow becomes symmetric at the fraction measurement point. This means that any measurement made on the diameter can be related to the cross section of the pipe in all directions. This is further explained in Pinguet [45].

In the case a Vx meter is placed far away from the well head a horizontal flow regime could establish in the pipeline in between. When this horizontal flow reaches the meter the horizontal flow pattern cannot always develop into an established vertical flow regime before it enters the venturi. A 'blind T' configuration is used below the venturi inlet as a weak flow conditioner aiming at homogenizing the liquids before entering the venturi section. Figure 4.4 shows a better representation of how to mixing works in such a 'blind T' configuration.

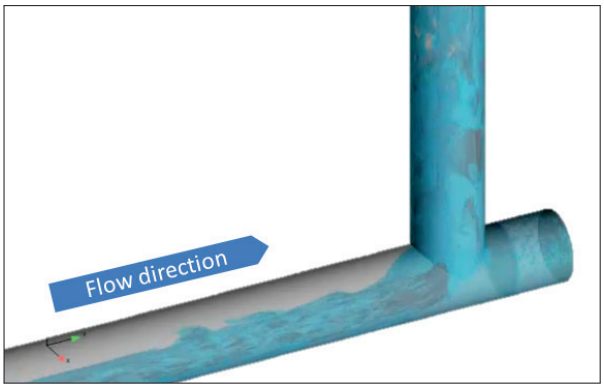

Figure 4.4: 3D model on how stratified horizontal flow regime is mixed efficiently before entering the venturi section due to the "Blind T" configuration.

The venturi flow restriction together with the blind T has an influence on the flow regime. While both those components act as flow conditioners, flow regimes can be significantly more complex in the meter compared to a pipe where longer flow distances allow for a better establishment of flow. This is the reason why an accurate flow regime characterization is not possible with the meter.

DETECTION OF FLOW REGIMES WITH THE VX METER

The previous paragraph made clear that an accurate flow regime detection with the Vx meter is very difficult during field operations. Although, there are a few exceptions where it is quite easy to detect a specific flow regime, such as in the case of low frequency intermittent flow. This is shown in figure 4.5 which gives a 2 hour section of a production test.

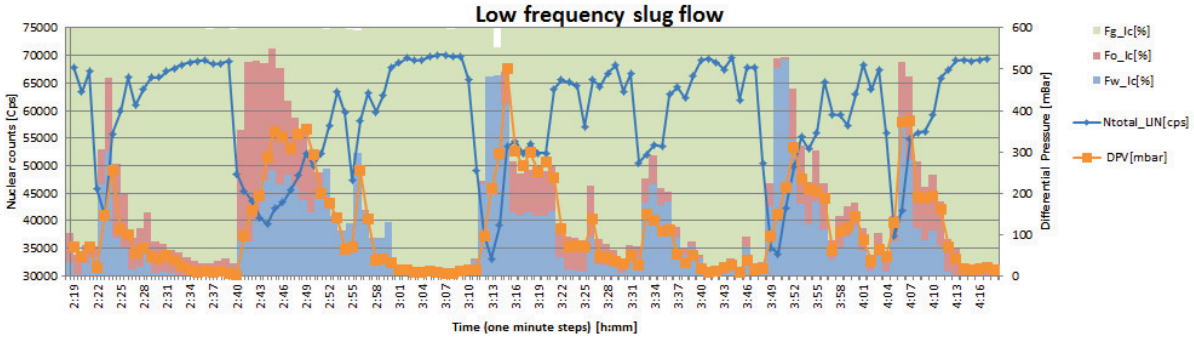

Figure 4.5: 2 hour time frame of a production test consisting the primary measurements of; Nuclear Counts, Differential Pressure, and the calculated phase fractions. The liquid fractions goes up from 0% to 80% with the differential pressure accross the venturi reaching near-zero values during periods shere only gas is pressent in the meter, which is a clear indication of intermittent flow.

Nonetheless, when another section (figure 4.6) is taken into account it can be seen how difficult a proper flow pattern detection usually is. One could observe constant parameters in the first hour. So a dispersed or separated flow can be defined, which brings the possibilities down to a bubble, mist or annular flow pattern. The gas fraction indicates an annular flow. However, this is not more than a best guess. In the second hour of figure 4.6, the flow regime is obviously turned into an intermittent flow which puts the suspicion into the direction of a slug or churn flow.

Conclusion It is possible to define with Vx meter data if the flow is a dispersed/separated flow or an intermittent flow. It is usually impossible to accurately define a flow pattern. However, there are cases where a

flow regime is easily detected, for example in the case of a low frequency slug flow, see figure .

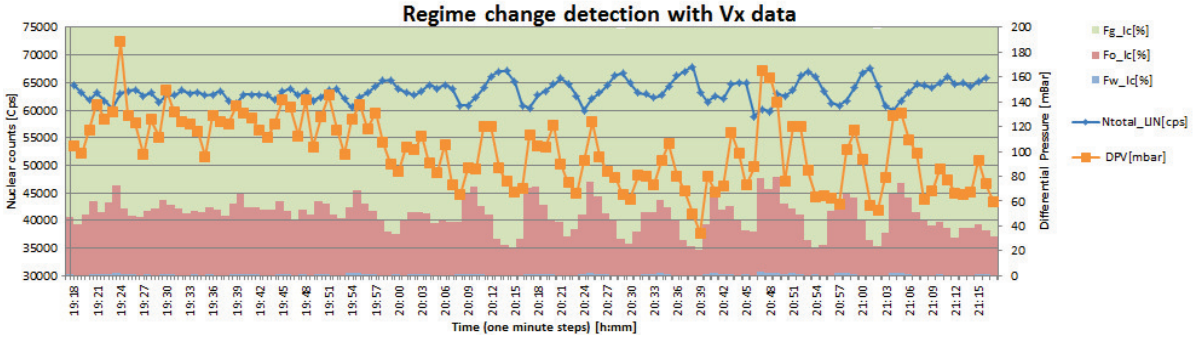

Figure 4.6: 2 hour time frame of a production test with a regime change. Consisting of the primary measurement of; Nuclear Counts and Differential Pressure, and the calculated phase fractions.

DETECTION OF FLOW REGIME CHANGES WITH THE VX METER

Despite the difficulties in defining accurate flow regimes, figure 4.6 shows us a tremendous ability of the dual gamma ray technology over conventional test separators. The ability to detect a flow regime transition directly. In the example it is without a doubt that around the time of 20:00 a flow regime change occurred, likely due to a reduction in flow rate as evidenced by the differential pressure reading, even though the flow regimes itself are not entirely certain.

Conclusion The Vx meter data can give valuable information whether a flow regime is constant or not.

4.1.3. STABLE FLOW

What is the definition of a stable or unstable state flow exactly and how are they recognized? How does this definition stands in relation with a stable flow? Before this question can be answered the definition should be clarified.

In systems theory, a system in a steady state has numerous properties that are unchanging in time. This means that for instance for the property p of a system, the partial derivative with respect to time should be zero:

$$\frac{\partial p}{\partial t} = 0$$

In production testing this never happens, there is always some change of the parameters over time so we cannot use the word "steady-state" flow. However, when the parameters over time are very robust with small disturbances, it can be defined as a stable flow. A stable flow means that the behavior of the production will continue into the future. In that case the pressure disturbance has reached far enough into the formation to allow determination of a representative information from the reservoir, which is essential for future decision making on the well. In a production test, a stable flow is not achieved until some time after the system is started or initiated. This initial situation is often identified as a transient state, start-up or warm-up period.

In the case of dispersed or separated flow it is quite easy to define stable flow. As the parameters give a continuous signal the operator should simply wait until the measurement parameters are fluctuating within the required spectrum. All operators have their own ad-hoc methodologies in order to define a stable flow.

These ad-hoc methodologies are originate from the time when only test separator data was available and, therefore, are not applicable for intermittent flow regimes, as test separators are not able to detect rapid variations in the nature of the flow.

This is a huge flaw in current production test duration determination, because a flow can be intermittent and still be a stable flow regime. This will be the case when parameters are slugging over time in a fixed frequency. It could also be the case that a slug or churn flow has several slug frequencies. Other names for this kind of stable flow are ”periodic flow” or ”developed flow”. With the current practices it is not possible to define such a stable developed flow.

Currently, in the case a production test has intermittent flow behavior, the operator will just guess on experience whether the production test can be concluded or not. At best, the decision will be made with the help of a moving average on the flow rates but this requires both experience and manual data analysis.

Fortunately, the Vx meter gives the opportunity to approach intermittent flow in a different way. As the high frequency data is obtained non-intrusively, there is much more information about the stability of the flow compared to a test separator. The system could be approached scholastically. It is possible, for example, to study the probability distribution of parameters over time. In an intermittent but stable flow (developed flow) the probability distribution of the parameters should remain constant over time.

Furthermore, signal analysis techniques can be applied on the data. It gives the ability to study the frequency of the parameters over time.

4.2. AVAILABLE TECHNIQUES TO PERFORM ON VX DATA

In this section applicable digital signal analysis techniques found in literature are introduced and explained.

4.2.1. SPECTRAL ANALYSIS ON FLOW PATTERNS IN LITERATURE

In chemical industries a lot of development is happening in compact reactor systems. This has triggered a demand for a comprehensive understanding of gas-liquid flow characteristics in tubes. As in a nuclear reactor it is essential to know what flow pattern is present in the cooling tubes for safety. Hence a lot of research has been done on developing techniques for flow pattern recognition by noise analysis (van der Hagen [29]). Most of those techniques can only be applied in a controlled environment with known parameters (van der Hagen and van der Voet [46], Van der Hagen and Hoogenboom [47], Suman *et al.* [48]).

It is impossible to use these techniques for an accurate flow pattern recognition in a production test, because the environment is far from controlled. However, the techniques proposed are ideally suited in evaluating whether an intermittent flow regime is deviating over time or not.

The following techniques proposed in literature will be used: the probability density function (PDF); the fast fourier transform (FFT) and signal filtering.

4.2.2. STATISTICAL ANALYSIS IN TIME DOMAIN

A very good tool in defining a flow pattern in time variant data, is with PDF analysis. Several researchers used this methodology in order to define flow patterns in gas-liquid multiphase flows (Jones Jr and Zuber [49], Jones Jr and Delhaye [50]). Different statistical moments like mean (m), standard deviation (r), and skewness (S) are used to characterize the PDF curves. While skewness indicates the degree of asymmetry of a distribution around its mean, the standard deviation represents the departure of data points from the average value. A bi-modal PDF, with multiple peaks, is usually an indication for an intermittent flow pattern. The ratio of the peak heights at low and higher values of a measured parameter can give an impression on the average frequencies present in an intermittent flow.

4.2.3. FREQUENCY DOMAIN ANALYSIS

Transforming the signal to the frequency domain is a great way to analyze the flow regime. Because this makes it possible to make a distinction between slug frequencies and noise van der Hagen [29].

A FFT is an algorithm to compute the discrete Fourier transform (DFT) and its inverse. Fourier analysis converts time (or space) to frequency and vice versa; a FFT rapidly computes such transformations by factorizing the DFT matrix into a product of sparse (mostly zero) factors.

In the present study the frequencies are presented as cycles per hour and the corresponding amplitudes the amount of frequency components. The slug frequency was evaluated from this representative mode of FFT and is denoted as Sf.

4.3. PROPOSED LOGICAL TESTS TO DEFINE A STABLE FLOW

In the previous section it became clear that it is possible to detect transitions between different flow regimes. Furthermore, by observing the Vx meter parameters over time it can be defined whether the flow regime is dispersed/separated or intermittent. Finally, in some cases even the actual flow regime can be defined. In this section an automatic method is proposed and explained in order to define a proper test duration for a production test. The algorithm is tested on numerous production tests with actual Vx meter data. Finally, the proposed methodology is compared with ad-hoc methods currently used in the industry to emphasize its

added value.

4.3.1. PREPARATION MEASURES

This section introduces the used parameters for analysis and how the Vx measurement data is processed.

PARAMETER SELECTION FOR ANALYSIS

The proposed analysis methods could be done on all the data parameters produced by the Vx meter. The most important parameters can be separated into raw measurements and calculated data:

Raw measurements:

- DPV: Differential pressure over the venturi.
- N32, N81 & N356: Nuclear counts of the source Barium 133 at different energy levels in keV.
- TL: Line Temperature
- PL: Line Pressure

Calculated data:

- q_o, q_w & q_g: Volumetric flow rates of individual phases. Both at line conditions and standard conditions.
- $\dot{m}_o$, $\dot{m}_w$ & $\dot{m}_g$: Mass flow rates of individual phases. Both at line conditions and standard conditions.

The calculated data is obtained with the help of models which need user input. The uncertainty on user input introduces an extra uncertainty on the calculated data. Faulty user input could be, for instance, a wrong water density due to an unexpected change in salinity over time. This is impossible with raw measurements. Hence only the raw measurement parameters are selected for the actual analysis.

Taking the raw measurements. Line Pressure (PL) and Line Temperature (TL) have a strong correlation with the reservoir itself. Those parameters can decrease or increase continuously over a whole production test. Which makes them not suitable for spectral analysis.

Nuclear counts are representing the composition of the fluid in the venturi section and is not affected by secondary influences. The counts from the $81keV$ energy level are mostly influenced by the mixture density and are thus represent a good indicator of variations in gas content. Also, this energy level is the least sensitive contrary to the high sensitive $32keV$ energy level. Therefore, the $81keV$ energy level is found most suitable for analysis.

Differential pressure (DPV) is also suitable for analysis. It represents the pressure drop over the convergence part in the venturi section and is thus a good indicator of total flow stability as well as of variations in gas content.

Conclusion The N81 and DPV raw data measurements are found to be the most suitable parameters for the spectral analysis. They are both used in the final methodology.

REPRESENTING VX METER PARAMETERS IN A SIGNAL

Digital spectral analysis techniques can only be done on discrete time signals (DTS). The Vx meter produces one data point per minute, so digital spectral analysis is possible.

In figure 4.7 an example is given of a DPV signal over the whole production test duration. This example clearly shows an intermittent flow behavior. In the first 600 minutes it can be seen that the flow regime is changing. However, in the last part of the production test it is visually impossible to state whether the flow is stable or not.

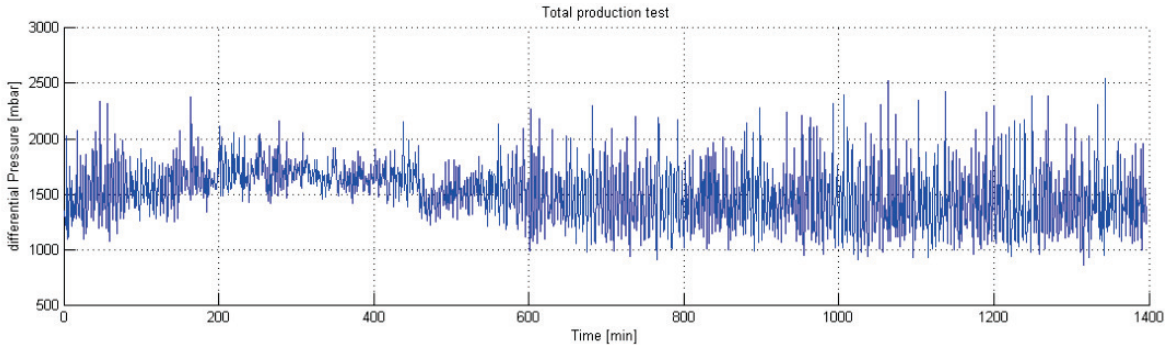

Figure 4.7: An example of a discrete time signal from a Vx meter. This signal represents the Differential Pressure over the whole production test.

4.3.2. TEST 1: ENSURE SIGNAL IS NOT DEVIATING OVER TIME

A production test which is not constant over time, is not stable. For a smart and simple way to detect this kind of deviation, the signal could be transformed to the frequency domain. This is done by cutting the signal in smaller segments of 120 minutes, considered to capture slow variations indicative of a long-term trend, avoid a bias from low-frequency variations and use a sufficient amount of data points for interpretation. See an example of such windowing on a N81 signal in figure 4.10. The window is shifted 15 minutes in time and a record of 120 minutes is taken. This is repeated over the whole production test signal. Finally, the separate records are transformed to the frequency domain with the help of the fast fourier transform (FFT). The first logical test can be performed:

Logic test 1 *When the frequency peaks surpass a threshold of 2000 components in the 0 to 2 cycles per hour range, the window is declared unstable. Having such frequency content in the signal indicates the presence of long-term trends in the measured data clearly indicating that the flow is not stable.*

Now two examples are given to show how the test reacts to an unstable or stable flow.

EXAMPLE 1: TEST 1 ON AN UNSTABLE FLOW

Figure 4.8 shows a clear example of a production test with an intermittent flow regime. The test clearly shows unstable behavior.

In this example the signal is deviating over time and the yellow window represents clearly an unstable flow moment in the production test.

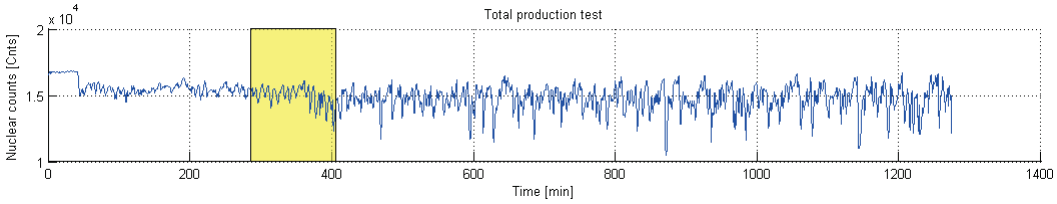

Figure 4.8: Example of a N81 signal deviating over time.

The signal records are transformed into the frequency domain by the FFT. The result of the yellow record in figure 4.8 being transformed to the frequency domain is shown in figure 4.9.

Now the actual test can be done. Note the enormous peak in the green window, which is the 0 to 2 cycles per hour range. Those peaks are clearly higher then 2000 frequency components. The threshold is represented with the red dashed line. Therefore, the flow regime in the yellow window in figure 4.8 is declared unstable.

The red line in figure 4.10 represents what the frequency peaks in the green window in figure 4.9 actually mean, after conversion back to the time domain. This is the information content after removing events corresponding to variations faster than 2 periods per hour. For a flow to be stable the red line should show a much more stable behavior.

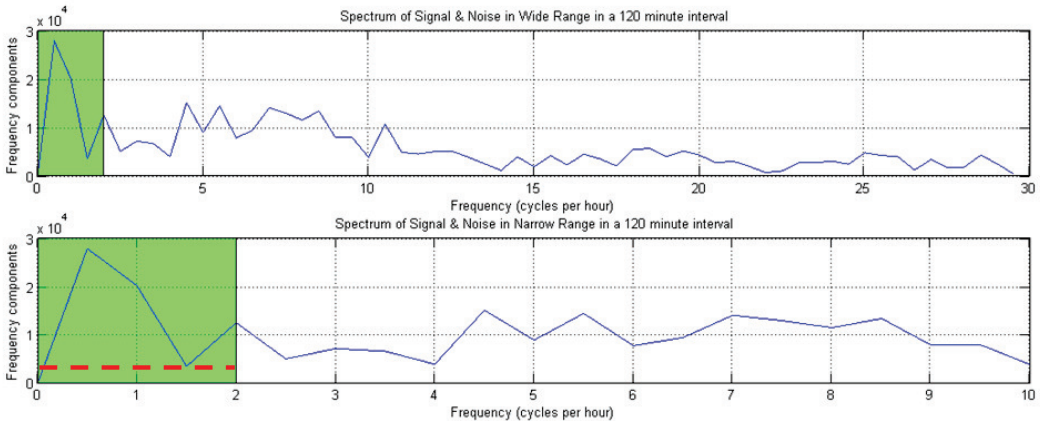

Figure 4.9: The yellow record in figure 4.8 transformed to the frequency domain.

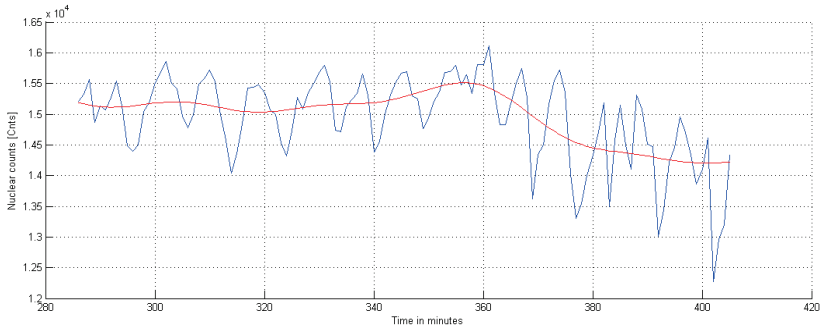

Figure 4.10: The blue line represents the yellow record in figure 4.8. The red line is a filtered version of the same record. It represents the frequency present in the green window in figure 4.9

Figure 4.11 is exactly the same as figure 4.9 however the complete production test is plotted. Every 15 minute timestep is another record of 120 minutes. The figure shows that very often there are high peaks in the 0 to 2 cycles per hour range, which indicates that this production test example is generally unstable and that no stable production has been achieved during the course of that test, even though it lasted for more than 20 hours.

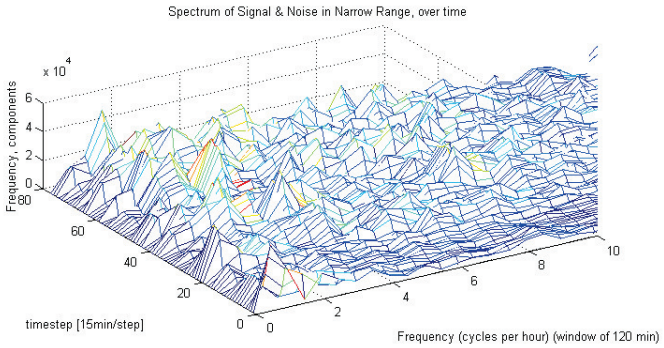

Figure 4.11: Frequency analysis as in figure 4.9 but over the whole production test

EXAMPLE 2: TEST 1 ON A STABLE FLOW

Example 2 again consists of an intermittent flow regime. However in this case there is stable flow behavior. Test 1 is able to show that to us. In figure 4.12 the whole production test is shown.

Again records of 120 minutes are taken from the signal and converted to the frequency domain. This is shown in figure 4.13. Now test 1 can be applied. The frequencies in the 0 to 2 cycles per hour range are clearly below the stated threshold (red dashed line) of 2000 frequency components and most of the fluctuations

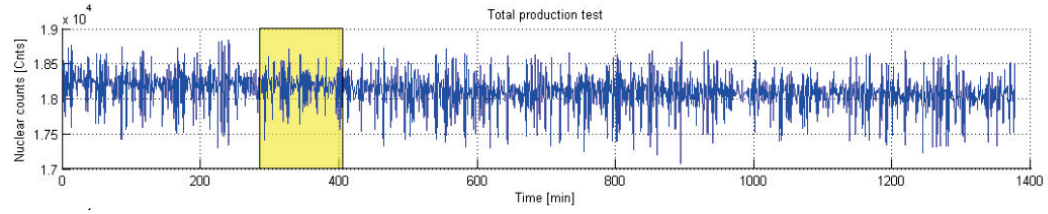

Figure 4.12: Example of a stable but intermittent N81 signal over time

actually correspond to high-frequency variations around an otherwise stable average. Therefore the record can be declared stable.

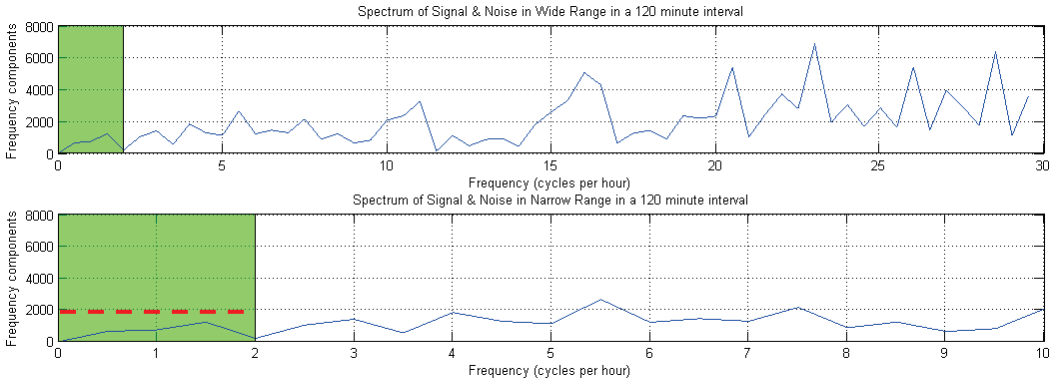

Figure 4.13: The yellow record in figure 4.12 transformed to the frequency domain.

Figure 4.15 shows the frequency domain of all the records over time. It shows that that the frequency is very low in the 0 to 2 cycles per hour range over the whole production test.

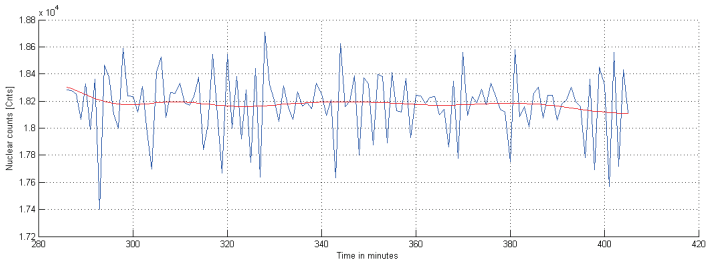

Figure 4.14: The blue line represents the yellow record in figure 4.12. The red line is a filtered version of the same record. It represents the frequency present in the green window in figure 4.9

Just as in example 1, the signal is filtered with a band-pass shown on the green range in figure 4.13. It can be observed that, contrary to example 1, the red line in this case is almost horizontal. Which is a good indication that the flow is stable over time despite the visible fluctuations in the original signal.

4.3.3. TEST 2: STOCHASTIC ANALYSIS TO DEFINE STABLE SECTIONS OF A PRODUCTION TEST

The second test is a stochastic approach in the time domain. It became clear in the former sections that taking the PDF over a production test signal does not always give a decisive answer on the actual flow pattern. However, the PDF is still very characteristic for a specific flow regime and comparing the PDF from different time windows will give us an idea whether the flow regime is stable or not.

As the distribution of the PDF is not known, a kernel density estimate (KDE) is necessary to approach the PDF. The KDE is modeled based on the work of Botev *et al.* [51].

The test consists of different steps. The first step uses the same window records as in section 4.3.2. Then, for every record of 120 minutes the PDF is taken. The distribution of the PDF is an unknown factor and deviating per flow regime. The PDF gives a unique flow signature in the case of intermittent flow. The distribution

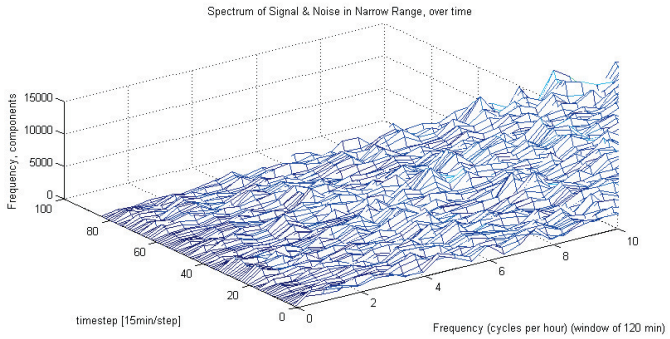

Figure 4.15: Frequency analysis as in figure 4.13 over the whole production test

of the PDF is, then, unknown and it can only be found with a histogram, or a Kernel Density estimate. See figure 4.16 for an example of this process.

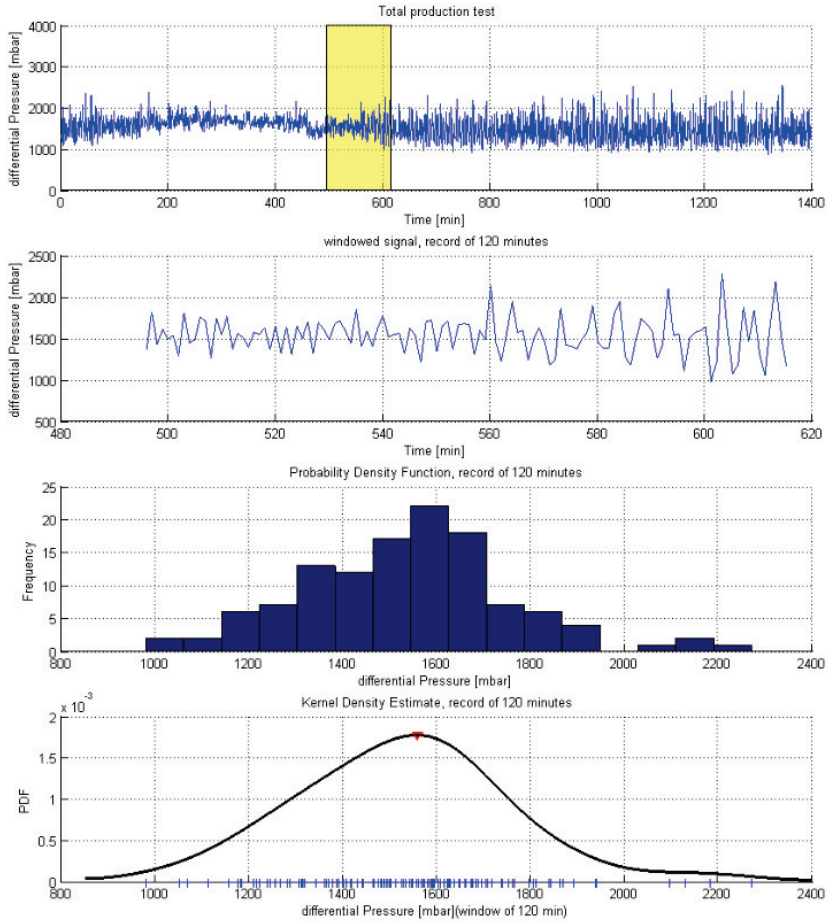

Figure 4.16: The same example as figure 4.7. In this figure the PDF has been analyzed on a specific window record of 120 minutes.

The second step is to take this PDF for all the time steps every 15 minutes and plot it over time. Then the location of the moving peaks of the PDF are identified over time. These moving peaks tell a lot about the flow stability. In the case peaks are deviating over time or (dis)appearing the flow is most likely unstable. Now the second logical test can be done.:

Logic test 2 *Compare the PDF on a 120 minute window record with the previous record and calculate the difference. IF: the difference of the DPV is below 5%. AND: N81 is below 2%. THEN: the flow is declared stable.*

Now an example is given to show how the test reacts on an example with a flow regime transition.

EXAMPLE 3: TEST 2 ON A FLOW REGIME TRANSITION.
In figure 4.17 test 2 is performed on a production test with a flow regime transition period. In the top graphs the signal of the N81 and DPV parameters are shown. In the second graphs the PDF is plotted for all the time steps. This way of plotting shows very clear where the flow regime is constant or in transition. In the third graph only the peaks of the PDF (global as well as local peaks) are shown for each timestep to clarify the behavior of the PDF over time. Finally, in the bottom graph test 2 is performed. The difference of the location of a PDF peak is taken between 2 subsequent records of the parameters. This difference is plotted with the green line. The red dashed line shows the requested threshold for a stable flow. The range where the green N81 and DPV graphs are both below the requested threshold is declared stable.

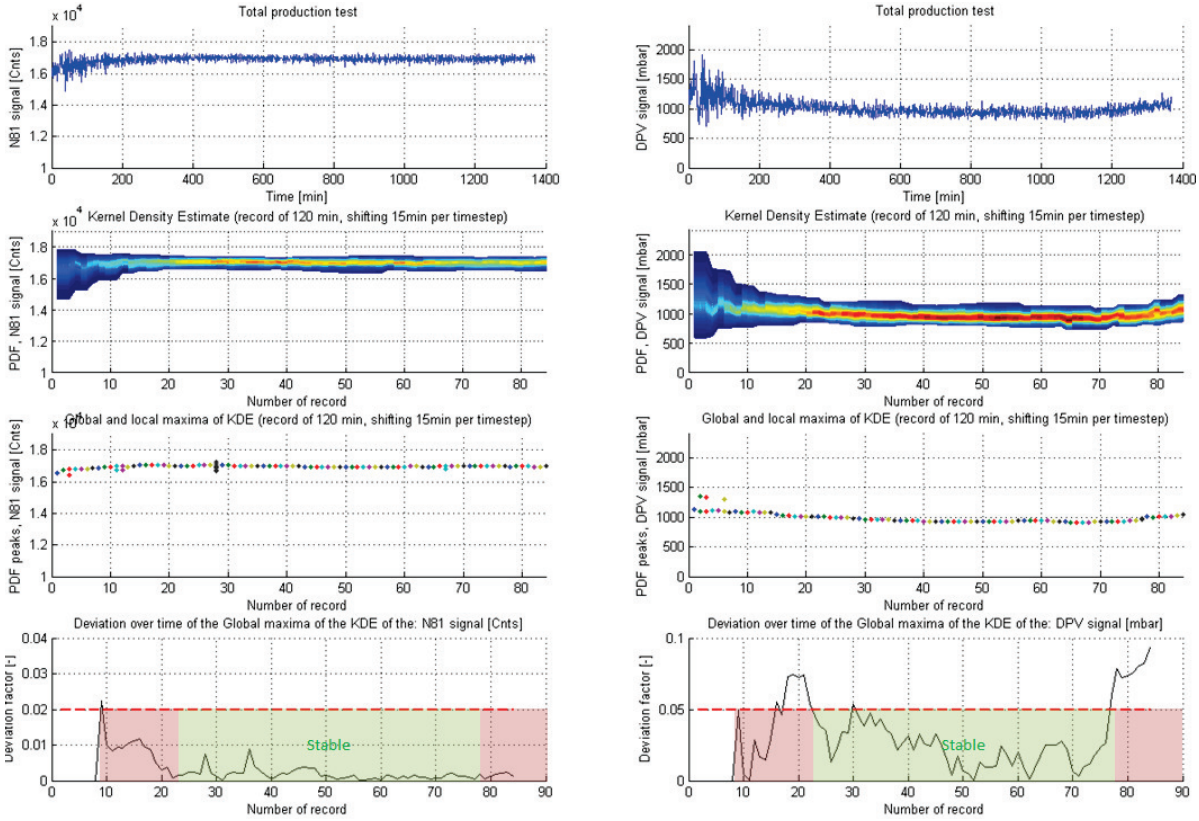

Figure 4.17: An example of test 2 performed on both a N81 and DPV signal.

The test on the example in figure 4.17 concludes that the flow regime was stable between time-step 24 (360 minutes) and 76 (1140 minutes) where the stability criteria is satisfied both on the differential pressure and N81 records.

4.3.4. TEST 3: LOOK FOR SLUG FLOW INDICATIONS

Generally it is impossible to define the exact flow pattern in a production test. However, in some cases it is possible to define the flow pattern, in the case of a slug flow, for example. The third and last test is to define whether the flow regime is a clear slug flow under developed flow conditions or not. This interpretation looks for the presence of a clear periodicity in the signal, which is a characteristic of slug flow.

For this test the same transformation is used as in test one. However, in this test the frequencies in the 2 to 10 cycles per hour range are counted (6 to 30 minute periodicity).

Logic test 3 *Find frequency peaks above 10.000 components in the 2 to 10 cycles per hour range and check their continuity over time. If the peaks are constant over time then the flow could be defined as a stable developed slug flow.*

Now an example is given to show how the test reacts on an example with a stable developed slug flow regime.

EXAMPLE 4: DETECTION OF A DEVELOPED SLUG FLOW

In figure 4.18 an example is given of a production test with a developed slug flow. Test 3 should be able to reveal this. Just as in the previous test the signal is dived in 120 minute window records. Then with the help of the FFT the signal records are transformed to the frequency domain. Now, the second test can be applied. If there are peaks which surpass 10.000 components in the 2 to 10 cycles per hour range then there is sluggy behavior. Figure 4.18 shows a clear peak above 10.000 components.

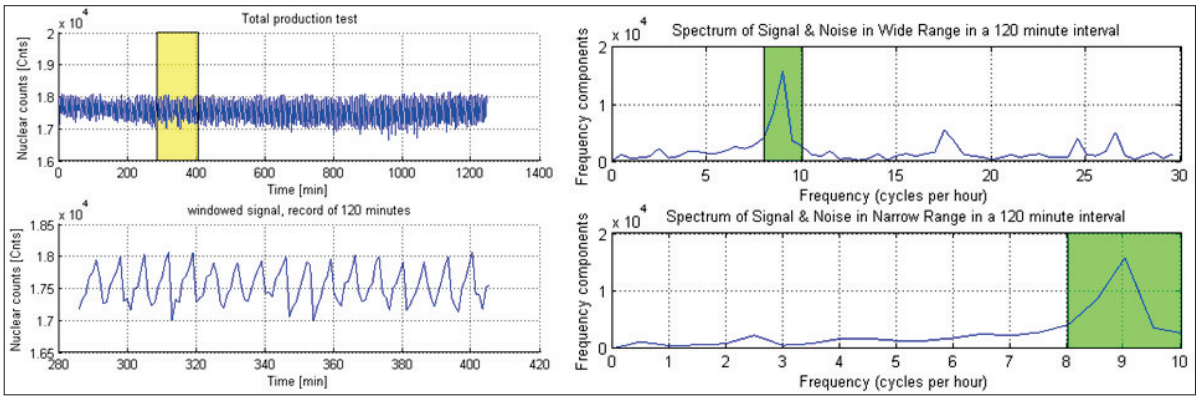

Figure 4.18: Frequency analysis on a 120 minute window record of a N81 signal.

When sluggy behavior is defined the next step is to check the behavior of the peak over time. This is done in figure 4.19. The graphs show a clear peak which stays constant over time. This is the proof that there is a developed slug flow of 9 cycles per hour. So the test can be declared stable.

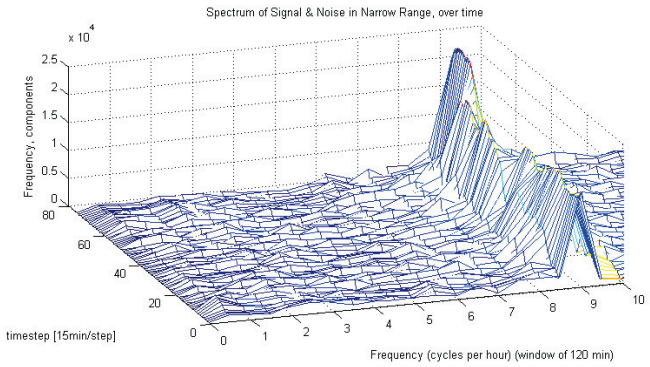

Figure 4.19: The frequency analysis in figure 4.18 done over the whole production test.

In the case there is a stable developed slug flow the slugs could be counted with using a band-pass filter around the frequency peak. See figure 4.20. The zero crossing of the green graph could be used as a counter.

4.4. RESULTS AND DISCUSSION

The proposed algorithm in section 4.3 is tested on actual production test data. The required threshold in the algorithm are based on the analysis of 700 production tests. In appendix C six production test examples are given and the results are discussed. These examples represent the main types of behavior observed in the available data. 90% of the data is similar to case 2.

The analysis detects in most of the cases a stable flow regime at some point except for a few exceptions, case 5 is an example. This is due to the low flow rates during that production test. The differential pressure is in constant movement.

Case 3 shows that the frequency analysis can illustrate whether the fluctuations are influenced by a certain flow regime or just a representation of noise originated by other influences.

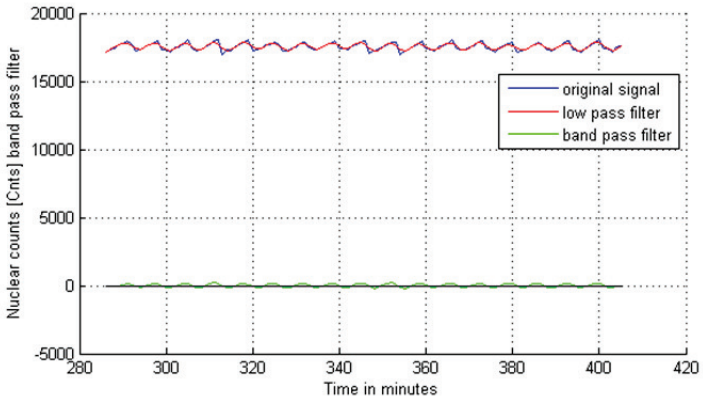

Figure 4.20: Bandpass filter on the green area in the frequency plot in fig 4.18

The third logic test works very well in case 4. A signal which looked like an unstable flow is in fact a high-frequency slugging well with a constant frequency.

4.5. CONCLUSION

In this chapter a new method based on the combination of several analyses in both the time and frequency domain has been proposed to define an optimal production test duration. This has two primary applications: to determine when a test can be ended as soon as flow stability has been achieved, yielding representative production test data; and to assist engineers in posterior analysis of production tests in order to automatically identify periods of stable flow truly representative of well performances. Such efficiency gains and automation are particularly important for production engineers, who have to manage the production of several hundreds of wells in parallel, and this amount will continue to grow according to Liddell *et al.* [7].

The method has the intention to make use of the extra data a Vx meter provides compared to conventional data.

- The algorithm gives more information on the stability of a flow regime then current practiced ad-hoc methods.
- The majority of all the analyzed production tests could have been concluded earlier with using the proposed algorithm.
- By representing the data with signal analysis techniques it is possible to observe flow regime transition.
- The presence of a slug flow can be detected and the associated frequency can automatically be extracted from the data.
- The selected thresholds should also be tested on other types of production test data before implementation. For example water or oil wells.

5

CONCLUSION AND RECOMMENDATIONS

The literature review and expert inquiry in chapter 2 showed that the use of a choke model is a good way to validate the flow rate measurements of a Vx meter during a production test. Furthermore, the review also showed that signal analysis on data gives more information about the stability of a flow than current conventional techniques.

The proposed choke model in chapter 3 is able to make a distinction between sub-critical and critical flow conditions. The model also can correct for the slippage of gas. Testing this choke model on a fixed choke in combination with actual Vx data showed that the accuracy is very satisfactory. This makes this choke model a better alternative than the current empirical choke models used. Considering flow rate validation, this choke model can be used to:

- Detect a drift in the DPV sensor output of the Vx meter.
- Detect the under- or overestimation of the gas rate calculated by the Vx meter
- Detect whether the meter is operating in the intended operation envelope or not.

The choke model needs an initial period in order to tune the overall discharge coefficient, or "tuning factor". It is recommended to define the ideal length of this tuning period by testing this choke model on a considerable amount of data sets. The choke model should only be tuned on a calibrated Vx meter.

In chapter 4 an algorithm is developed which uses the extra data a Vx meter delivers compared to data obtained with conventional test separators. The method is based on several analysis in both the time and frequency domain. This has two primary applications:

- Determine when a production test can be ended as soon as flow stability has been achieved, yielding representative production test data.
- Assist engineers in posterior analysis of production tests in order to automatically identify periods of stably flow truly representative of well performances.

The efficiency gains and automation given by the algorithm are of great importance for production engineers, as they generally have to manage a lot of wells per person.

- The algorithm gives more information of a flow regime then current practiced ad-hoc methods by operators.
- Testing the algorithm on actual production tests showed that he majority of the tests could be concluded earlier.
- By representing the data stochastic (PDF) it is possible to observe flow regime transition. It is in most cases impossible to define an exact flow pattern, however; observing a constant flow pattern, whatsoever the pattern actually is, represents a stable flow.
- By plotting the N81 into the frequency domain, a slug flow can be detected and the corresponding slug flow periodicity can easily be subtracted from the data.

The algorithm is tested on 700 gassy wells, it is recommended to test the algorithm on wells with more liquid before implementation in an automated fashion.

A

VX MULTIPHASE FLOW METER

This report focuses on flow rate data validation, on measurement data obtained by Vx multiphase flow meters. For readers without fundamental knowledge in dual gamma ray technology an compact overview is given about the technology behind the Vx meter. Pinguet [45] describes the Vx meter technology in more detail.

In short The principle of dual gamma ray technology is based on the mixture velocity and uses a venturi equation based on the same concept as a single phase flow. This venturi equation combines the differential-pressure measurement together with the mixture density measurement. The final flow rate values are obtained by combining the fraction measurements of each phase with the gas volume fraction (GVF) derived from a slip-law accounting for the slippage of gas. The fraction measurements are based on the attenuation of gamma rays through the fluid at the venturi throat.

Differential pressure (ΔP) The Vx meter contains of several parts, see figure A.1. The venturi section is a restriction in the flow to create a small permanent pressure drop, a venturi is designed in such a way that there is almost no permanent pressure drop. The small pressure drop is measured with the differential pressure transmitter, the DPV sensor.

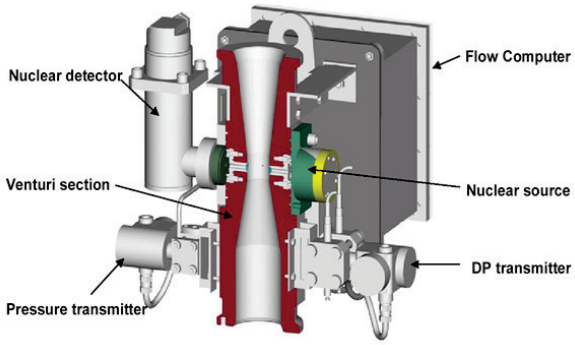

Figure A.1: Cross section of Vx meter.

Phase fractions (α_o, α_w & α_g) The three phase fractions of oil, water and gas are determined with gamma ray attenuation technology. A nuclear source is placed in such a way that a beam of nuclear gamma rays goes through the venturi throat. The chemical source is a Barium-133, selected because of its ideal half time. Barium-133 has, like any chemical source, a specific gamma ray spectrum shown in figure A.2. This spectrum is transmitted through the venturi throat by radiation and the numbers of gamma rays are counted at the detector. In the case of a vacuum in the venturi the detector would count the whole spectrum. When there is fluids in the venturi less gamma rays would arrive, which is called attenuation. The amount of gamma ray

attenuation depends on the specific fluid composition, called the Compton effect. See figure A.2 for examples of several fluid compositions and the corresponding attenuation.

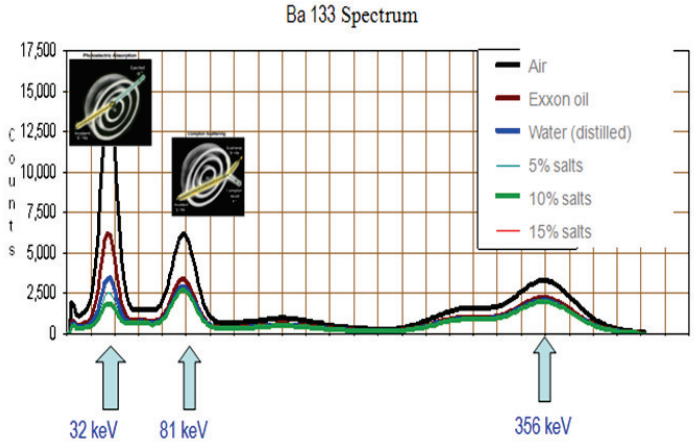

Figure A.2: Gamma ray spectrum of Barium-133.

Figure A.2 shows also that the height of the gamma ray spectrum differs per energy level. With the acquisition of the gamma ray attenuation at two energy levels; low energy, $le = 32keV$, and high energy, $he = 81keV$, it is possible to model the physical phenomena in the throat of the venturi, with the help of Lambert's law. With the help of a mathematical system which consists three 3 equations with each three unknowns, the phase fractions α_o,α_w & α_g can be calculated.

$$N^{le} = N_0^{le} e^{-D\left[\left(\mu_o^{le}\cdot\rho_o\cdot\alpha_o\right)+\left(\mu_w^{le}\cdot\rho_w\cdot\alpha_w\right)+\left(\mu_g^{le}\cdot\rho_g\cdot\alpha_g\right)\right]} \tag{A.1a}$$

$$N^{he} = N_0^{he} e^{-D\left[\left(\mu_o^{he}\cdot\rho_o\cdot\alpha_o\right)+\left(\mu_w^{he}\cdot\rho_w\cdot\alpha_w\right)+\left(\mu_g^{he}\cdot\rho_g\cdot\alpha_g\right)\right]} \tag{A.1b}$$

$$\alpha_o + \alpha_w + \alpha_g = 1 \tag{A.1c}$$

Here N_0^{le} & N_0^{he} are the total number of gamma rays at low- and high energy, coming from the source. N^{le} & N^{he} are the number of gamma rays detected at low- and high energy. μ_α is the mass attenuation which is unique per phase and known. ρ_α stands for the density per phase. The phase fractions are found by solving this system of 3 equations in A.1.

This solution can graphically be represented as a nuclear solution triangle, figure A.3. Initially, before the measuring of the multiphase fluid begins, a 100% oil, water and gas is subsequently flown through the meter in order to define the water, oil and gas points. Then, when the meters is working the operating point is measured. With the location of this operating point, in respect to the water, oil and gas point, the phase fractions of the fluid can be calculated.

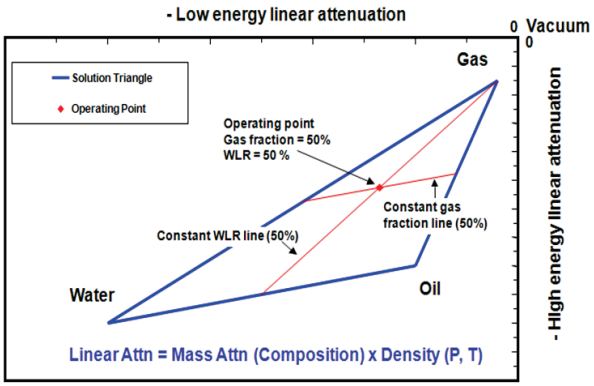

Figure A.3: Nuclear solution triangle.

Mixture density (ρ_m) When the phase fractions are known it is possible to obtain the mixture density. Together with the already known density of the different phases the expression in equation A.2 can be used.

$$\rho_m = \alpha_o \rho_o + \alpha_w \rho_w + \alpha_g \rho_g \tag{A.2}$$

Water liquid ratio (WLR) The WLR can be calculated directly from the phase fractions. As there is neglible slippage assumed between oil and water. This leads to equation A.3:

$$\text{WLR} = \frac{q_w}{q_l} = \frac{\alpha_w}{1-\alpha g} \tag{A.3}$$

Gas volume fraction (GVF) Contrary to oil and water, there is slippage between the liquid and gas phase. In order to calculate the gas cut (GVF) a slippage model is developed within Schlumberger and Framo. The model itself is not publicly available; however, the dependency of the model is shown in equation A.4.

$$\text{GVF} = fn\left(\frac{\rho_l}{\rho_g}, \frac{\eta_l}{\eta_g}, \alpha_g\right) \leq 1 \tag{A.4}$$

Mixture mass flow rate ($\dot{m}_m$) With the Differential pressure ΔP and mixture density ρ_m known, the total mass flow rate can be calculated. The expression to do so is based on Bernoulli's venturi equation for multiphase flow. The equation has some extra terms for the Vx meter, see equation A.5.

$$\dot{m}_m = \frac{C_{Re}\epsilon}{\sqrt{1-\beta^4}} \frac{\pi}{4} d^2 S_f \sqrt{2\Delta P \rho_m} \tag{A.5}$$

The discharge coefficient C_{Re}, unique for any meter, based on the Reinolds Re number. The expansibility factor ϵ which is different for gas or oil wells and the shape factor S_f.

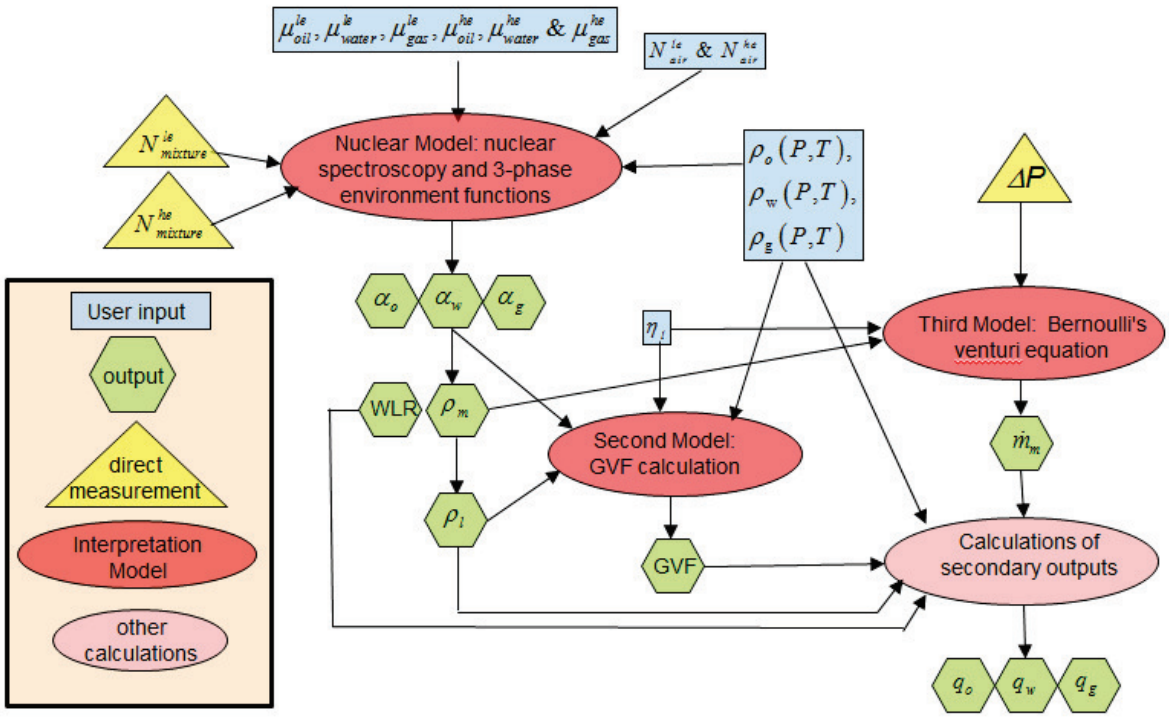

Figure A.4: Vx meter, calculation models.

Volumetric phase flow rates at local conditions ($q_{o,lc}, q_{w,lc}$ & $q_{g,lc}$) At this point all the meter's primary outputs are produced: mixture density, total mass flow rate, WLR and GVF. The secondary outputs (the phase flow rates at line conditions) are derived using the following approach:

$$\begin{aligned} q_m &= \frac{\dot{m}_m}{\rho_g\,(\mathrm{GVF}) + \rho_l\,(1-\mathrm{GVF})} \\ q_g &= GVF \cdot q_m \\ q_l &= \frac{\dot{m}_m - \dot{m}_g}{\rho_l} \\ q_o &= (1-\mathrm{WLR}) \cdot q_l \\ q_w &= \mathrm{WLR} \cdot q_l \end{aligned} \tag{A.6}$$

These are the volumetric flow rates at local conditions. The last step is to convert these values to standard conditions. This can be done with black oil correlations for example such as

Figure A.4 gives the complete overview of how user input, output, direct measurements and the interpretation models are in relation with each other.

Vx meter in operations The Vx meter can be installed permanently in a production system, this variant is called the PhaseWatcher. The mobile variant of the Vx meter, the PhaseTester, can be used for well testing. See figure A.5 for operational examples.

Figure A.5: Example of a permanent installed Vx meter (PhaseWatcher) and mobile Vx meter (PhaseTester).

B

CHOKE MODEL: MATHEMATICAL DERIVATION

In this appendix all the model formulations of the choke model presented in chapter 3 are derived step by step.

B.1. BALANCE EQUATIONS

The same approach as in Jansen [30] is used. Experiments have determined that the majority of energy dissipation in a restriction occurs in the region of diverging streamlines (between point 3 and 4 in figure 3.1), whereas in the converging region (between point 1 and 3 in figure 3.1) the flow experiences only a small friction loss. Therefore, between point 1, the pipe inlet, and point 3, the vena contracta , neglible friction and gravity losses are assumed. Hence, the predominant pressure term is acceleration. Now, the steady-state mass and momentum balances can be written as follows.

Mass balance:

$$\underbrace{A\rho v}_{mass\ rate\ in} \underbrace{-\left(A+\frac{\partial A}{\partial s}\right)\left(\rho+\frac{\partial \rho}{\partial s}\right)\left(v+\frac{\partial v}{\partial s}\right)}_{mass\ rate\ out}=0 \tag{B.1}$$

Momentum balance:

$$\begin{aligned}\underbrace{A\rho v^2}_{momentum\ rate\ in} \underbrace{-\left(A+\frac{\partial A}{\partial s}\right)\left(\rho+\frac{\partial \rho}{\partial s}\right)\left(v+\frac{\partial v}{\partial s}\right)^2}_{momentum\ rate\ out} + \underbrace{Ap}_{left\ axial\ force} \\ + \underbrace{\left(p+\frac{1}{2}\frac{\partial p}{\partial s}ds\right)\left(\frac{\partial A}{\partial s}ds\right)}_{axial\ force\ along\ the\ pipe} \underbrace{-\left(A+\frac{\partial A}{\partial s}\right)\left(p+\frac{\partial p}{\partial s}ds\right)}_{right\ axial\ force}=0\end{aligned} \tag{B.2}$$

Here A is the area of the intersections of the flow line. ρ represents the density of the fluid, v is the velocity. p is the pressure term and s is the length along the converging part of the pipe.

An extra term is introduced in the momentum balance to account for the axial component of the force resulting from pressure on the pipe wall compared to a mass balance on a pipe without a restriction. Expanding the equations B.1 and B.2, then dropping all the terms higher than first order results in the following equations:

$$\frac{d\left(A\rho v\right)}{ds}=0 \tag{B.3}$$

$$A\rho v\frac{dv}{ds}+\frac{d\left(A\rho v\right)}{ds}v=-A\frac{dp}{ds} \tag{B.4}$$

Combining B.3 & B.4 results in the final momentum balance equation.

$$\frac{dp}{ds}=-\rho v\frac{dv}{ds} \tag{B.5}$$

B.2. POLYTROPIC FLOW ASSUMPTION

Just as in Jansen [30], Ros [32], Al-Safran and Kelkar [38], Perkins [39], Sachdeva *et al.* [40] the equation of state for the gas is modeled based on the assumption that polytropic behavior exists in the mixture, which is a thermodynamical term which means; in between isothermal and isotropic. In a single-phase gas, isentropic flow is assumed, to account for the temperature drop in the choke. In multi-phase flow the temperature drops less, because the surrounding liquid adsorbs rapidly the generated heat of the compressed gas. Polytropic assumptions can account for that process. The relationship between pressure and gas density under polytropic conditions is given by:

$$\frac{p}{\rho_g^n}=C \tag{B.6}$$

Here n is the polytropic expansion coefficient, defined as follows by Ros [32]:

$$n=1+\frac{x_g(c_{pg}-c_{vg})}{x_g c_{vl}+(x_g-1)c_{vl}} \tag{B.7}$$

Here x_g is defined as the flowing mass fraction of gas (or gas quality) at the throat (vena contracta) of the choke. The specific heat capacities[1] are defined as follows: c_{pg}[2] & c_{vg}[3] are the specific heat capacities for the gas at constant pressure and volume respectively, c_{vL} is the specific heat capacity for the liquid at constant volume.

With equation B.7 it can be clearly shown how the polytrophic flow assumption actually works. In the case $x_g = 1$ is taken, there is a singlephase gas flow and n will be the same as $\frac{c_p}{c_v}$ which corresponds to isentropic flow. Whereas $x_g = 0$ is taken, a 100 % liquid flow, n goes to 1 which corresponds with isothermal behavior.

Polytropic expansion According to Jansen [30] temperature and pressure can be related with the help of the polytropic expansion coefficient:

$$\frac{p^{\frac{n-1}{n}}}{T_{abs}}=C \tag{B.8}$$

This relation can be used to derive the polytropic Bernoulli equation.

B.3. SUB-CRITICAL MASS FLOW RATE

From here on, the derivation deviates from the method proposed in Jansen [30] as the slippage of gas is going to be included. An approach to do this is suggested in Al-Safran and Kelkar [38]. Again, the momentum balance as derived in B.5 serves as the starting point. The balance equation considers acceleration and pressure forces (and discards friction and gravity effects).

$$\frac{1}{\rho_{ms}}\frac{dp}{ds}=-v_{ms}\frac{dv}{ds} \tag{B.9}$$

[1] *Heat capacity:* The measurable physical quantity of heat energy to change the temperature of an object by a given amount. The heat capacity is expressed in $\left[\frac{J}{K}\right]$.

Specific heat capacity: The heat capacity per unit mass of a material. This is expressed in $\left[\frac{J}{(kg*K)}\right]$.

[2] *Specific heat capacity at constant volume c_v:* A unit increase in temperature of a unit of mass of an object at constant volume (and increasing pressure) results in an increase of energy with c_v.

[3] *Specific heat capacity at constant pressure c_p:* A unit increase in temperature of a unit of mass of an object at constant pressure (and increasing volume) results in an increase of energy with c_p.

B.3.1. INVERSE MIXTURE DENSITY INCLUDING SLIP

In order to solve equation B.9 an expression is needed for the inverse mixture density $\frac{1}{\rho_{ms}}$ which takes slippage of gas into account. The mixture momentum density is described in Schüller *et al.* [41] and used in Al-Safran and Kelkar [38]. If slip is included the equation can be written as follows:

$$\frac{1}{\rho_{ms}} = \left[\frac{x_g}{\rho_g} + \frac{Rx_l}{\rho_l}\right]\left[x_g + \frac{x_l}{R}\right] \tag{B.10}$$

Where R stands for the slip ratio which can be defined in several ways, depending on the assumptions taken. This formula can easily be verified, in the case the slippage of gas is disregarded, $R = 1$ should be chosen. In that case B.10 becomes the original 'no-slip inverse mixture density' relation as used in, Jansen [30], Sachdeva *et al.* [40]:

$$\frac{1}{\rho_{mn}} = \left[\frac{x_g}{\rho_g} + \frac{1 * x_l}{\rho_l}\right]\left[x_g + \frac{x_l}{1}\right] = \left[\frac{x_g}{\rho_g} + \frac{x_l}{\rho_l}\right] \tag{B.11}$$

B.3.2. MATHEMATICAL DERIVATION OF SUB-CRITICAL MASS FLOW RATE

The inverse mixture density equation B.10 is substituted into the left side of the momentum balance equation B.9. Integration from s_1 to s_3 results in:

$$\begin{aligned}\int_{s_1}^{s_3} \frac{1}{\rho_{ms}}\frac{dp}{ds}ds &= \int_{s_1}^{s_3}\left(\left[\frac{x_g}{\rho_g} + \frac{Rx_l}{\rho_l}\right]\left[x_g + \frac{x_l}{R}\right]\right)\frac{dp}{ds}ds \\ &= \int_{s_1}^{s_3}\left(\frac{x_g^2}{\rho_g} + \frac{Rx_lx_g}{\rho_l} + \frac{x_lx_g}{R\rho_g} + \frac{x_l^2}{\rho_l}\right)\frac{dp}{ds}ds\end{aligned} \tag{B.12}$$

Then, the relationship between pressure and density of gas is substituted in equation B.6:

$$\begin{aligned}&\int_{s_1}^{s_3}\left(\frac{x_g^2 C^{\frac{1}{n}}}{p^{\frac{1}{n}}} + \frac{Rx_lx_g}{\rho_l} + \frac{x_lx_gC^{\frac{1}{n}}}{Rp^{\frac{1}{n}}} + \frac{x_l^2}{\rho_l}\right)\frac{dp}{ds}ds \\ &= x_g^2 C^{\frac{1}{n}}\int_{p_1}^{p_3} p^{-\frac{1}{n}}dp + \frac{Rx_lx_g}{\rho_l}\int_{p_1}^{p_3} 1dp + \frac{x_lx_gC^{\frac{1}{n}}}{R}\int_{p_1}^{p_3} p^{-\frac{1}{n}}dp + \frac{x_l^2}{\rho_l}\int_{p_1}^{p_3} 1dp \\ &= x_g^2 C^{\frac{1}{n}}\frac{n}{n-1}p^{\frac{n-1}{1}}\Big|_{p_1}^{p_3} + \frac{Rx_lx_g}{\rho_l}p\Big|_{p_1}^{p_3} + \frac{x_lx_gC^{\frac{1}{n}}}{R}\frac{n}{n-1}p^{\frac{n-1}{1}}\Big|_{p_1}^{p_3} + \frac{x_l^2}{\rho_l}p\Big|_{p_1}^{p_3} \\ &= \left(\frac{x_g^2}{\rho_g}\frac{n}{n-1} + R\frac{x_lx_g}{\rho_l} + \frac{1}{R}\frac{x_lx_g}{\rho_g}\frac{n}{n-1} + \frac{x_l^2}{\rho_l}\right)p\Big|_{p_1}^{p_3}\end{aligned} \tag{B.13}$$

Integrating the right side of the momentum balance in equation B.9 and combining the result of equation B.13 gives the polytropic Bernoulli equation for gas-liquid flow, including the slippage of the gas phase:

$$\begin{aligned}&\left(\frac{x_g^2}{\rho_{g1}}\frac{n}{n-1} + R\frac{x_lx_g}{\rho_l} + \frac{1}{R}\frac{x_lx_g}{\rho_{g1}}\frac{n}{n-1} + \frac{x_l^2}{\rho_l}\right)p_1 + \frac{1}{2}v_{ms,1}^2 \\ &\qquad = \left(\frac{x_g^2}{\rho_{g3}}\frac{n}{n-1} + R\frac{x_lx_g}{\rho_l} + \frac{1}{R}\frac{x_lx_g}{\rho_{g3}}\frac{n}{n-1} + \frac{x_l^2}{\rho_l}\right)p_3 + \frac{1}{2}v_{ms,3}^2\end{aligned} \tag{B.14}$$

The mixture slip velocity v_{ms} is rewritten in terms of the mass flow rate $\dot{m}$:

$$\frac{1}{2}v_{ms}^2 = \frac{1}{2}\left(\frac{\dot{m}}{A\rho_{ms}}\right)^2 = \frac{1}{2}\frac{\dot{m}^2}{A^2\rho_{ms}^2} \tag{B.15}$$

Now, with the aid of equation B.15 the Bernoulli equation B.14 can be rewritten as follows:

$$\left(\frac{x_g^2}{\rho_{g1}}\frac{n}{n-1}+R\frac{x_l x_g}{\rho_l}+\frac{1}{R}\frac{x_l x_g}{\rho_{g1}}\frac{n}{n-1}+\frac{x_l^2}{\rho_l}\right)p_1-\left(\frac{x_g^2}{\rho_{g3}}\frac{n}{n-1}+R\frac{x_l x_g}{\rho_l}+\frac{1}{R}\frac{x_l x_g}{\rho_{g3}}\frac{n}{n-1}+\frac{x_l^2}{\rho_l}\right)p_3 = \frac{1}{2}\dot{m}^2\left(\frac{1}{A_3^2\rho_{ms,3}^2}-\frac{1}{A_1^2\rho_{ms,1}^2}\right) \tag{B.16}$$

Then, equation B.16 can be rewritten again with the help of equation B.10:

$$\frac{x_g^2}{\rho_{g1}}\frac{n}{n-1}p_1+\frac{1}{R}\frac{x_l x_g}{\rho_{g1}}\frac{n}{n-1}p_1-\frac{x_g^2}{\rho_{g3}}\frac{n}{n-1}p_3-\frac{1}{R}\frac{x_l x_g}{\rho_{g3}}\frac{n}{n-1}p_3+R\frac{x_l x_g}{\rho_l}p_1+\frac{x_l^2}{\rho_l}p_1-R\frac{x_l x_g}{\rho_l}p_3-\frac{x_l^2}{\rho_l}p_3 = \frac{1}{2}\dot{m}^2\left(\frac{1}{A_3^2\rho_{ms,3}^2}-\frac{1}{A_1^2\rho_{ms,1}^2}\right) \tag{B.17}$$

$$\left[\frac{x_g n}{n-1}\left(\frac{p_1}{\rho_{g1}}-\frac{p_3}{\rho_{g3}}\right)+R\frac{x_l}{\rho_l}\left(p_1-p_3\right)\right]\left[x_g+\frac{x_l}{R}\right] = \frac{1}{2}\frac{\dot{m}^2}{A_3^2\rho_{ms,3}^2}\left(1-\frac{A_3^2\rho_{ms,3}^2}{A_1^2\rho_{ms,1}^2}\right) \tag{B.18}$$

Subsequently, the right inverse mixture density expressions equation B.10 can be substituted to define the pressure ratio in terms of $p_r = p_3/p_1$. Together with the relation $\frac{1}{\rho_{g,3}} = \left(\frac{1}{\rho_{g,1}}\right)p_r^{-\frac{1}{n}}$, the following expression is found:

$$\left[\frac{x_g n}{n-1}\frac{p_1}{\rho_{g1}}\left(1-\frac{p_3\rho_{g1}}{p_1\rho_{g3}}\right)+R\frac{x_l}{\rho_l}p_1\left(1-\frac{p_3}{p_1}\right)\right]\left[x_g+\frac{x_l}{R}\right] = \frac{1}{2}\frac{\dot{m}^2}{A_3^2}\left[\frac{x_g}{\rho_{g3}}+R\frac{x_l}{\rho_l}\right]^2\left[x_g+\frac{x_l}{R}\right]^2\cdot\left(1-\left(\frac{\left[\frac{x_g}{\rho_{g1}}+R\frac{x_l}{\rho_l}\right]\left[x_g+\frac{x_l}{R}\right]}{\left[\frac{x_g}{\rho_{g3}}+R\frac{x_l}{\rho_l}\right]\left[x_g+\frac{x_l}{R}\right]}\right)^2\left(\frac{A_3}{A_1}\right)^2\right) \tag{B.19}$$

$$\left[\frac{x_g n}{n-1}\frac{p_1}{\rho_{g1}}\left(1-p_r^{\frac{n-1}{n}}\right)+R\frac{x_l}{\rho_l}p_1\left(1-p_r\right)\right] = \frac{1}{2}\frac{\dot{m}^2}{A_3^2}\left[\frac{x_g}{\rho_{g1}}p_r^{-\frac{1}{n}}+R\frac{x_l}{\rho_l}\right]^2\left[x_g+\frac{x_l}{R}\right]\cdot\left(1-\left(\frac{\left[\frac{x_g}{\rho_{g1}}+R\frac{x_l}{\rho_l}\right]}{\left[\frac{x_g}{\rho_{g1}}p_r^{-\frac{1}{n}}+R\frac{x_l}{\rho_l}\right]}\right)^2\left(\frac{A_3}{A_1}\right)^2\right) \tag{B.20}$$

Now, $\alpha = (Rx_l\rho_{g,1})/(x_g\rho_l)$ is defined to decrease the complexity of the expression:

$$\left[\frac{x_g n}{n-1}\frac{p_1}{\rho_{g1}}\left(1-p_r^{\frac{n-1}{n}}\right)+R\frac{x_l}{\rho_l}p_1\left(1-p_r\right)\right]\cdot\frac{\rho_{g1}}{x_g} = \left[\frac{1}{2}\frac{\dot{m}^2}{A_3^2}\left[\frac{x_g}{\rho_{g1}}p_r^{-\frac{1}{n}}+R\frac{x_l}{\rho_l}\right]^2\left[x_g+\frac{x_l}{R}\right]\cdot\left(1-\left(\frac{\left[\frac{x_g}{\rho_{g1}}+R\frac{x_l}{\rho_l}\right]}{\left[\frac{x_g}{\rho_{g1}}p_r^{-\frac{1}{n}}+R\frac{x_l}{\rho_l}\right]}\right)^2\left(\frac{A_3}{A_1}\right)^2\right)\right]\cdot\frac{\rho_{g1}}{x_g} \tag{B.21}$$

$$\left[\frac{n}{n-1}p_1\left(1-p_r^{\frac{n-1}{n}}\right)+R\frac{x_l}{\rho_l}\frac{\rho_{g1}}{x_g}p_1\left(1-p_r\right)\right] = \frac{1}{2}\frac{\dot{m}^2}{A_3^2}\frac{\rho_{g1}}{x_g}\left[p_r^{-\frac{1}{n}}+R\frac{x_l}{\rho_l}\frac{\rho_{g1}}{x_g}\right]^2\left[x_g+\frac{x_l}{R}\right]\cdot\left(1-\left(\frac{\left[1+R\frac{x_l}{\rho_l}\frac{\rho_{g1}}{x_g}\right]}{\left[p_r^{-\frac{1}{n}}+R\frac{x_l}{\rho_l}\frac{\rho_{g1}}{x_g}\right]}\right)^2\left(\frac{A_3}{A_1}\right)^2\right) \tag{B.22}$$

$$\left[\frac{n}{n-1}p_1\left(1-p_r{}^{\frac{n-1}{n}}\right)+\alpha p_1\left(1-p_r\right)\right] = \frac{1}{2}\frac{\dot{m}^2}{A_3^2}\frac{\rho_{g1}}{x_g}\left[p_r{}^{-\frac{1}{n}}+\alpha\right]^2\left[x_g+\frac{x_l}{R}\right]\cdot\left(1-\left(\frac{\left[p_r{}^{-\frac{1}{n}}+\alpha\right]}{[1+\alpha]}\right)^2\left(\frac{A_3}{A_1}\right)^2\right) \tag{B.23}$$

Rearranging results in the following expression:

$$\dot{m}^2 = \frac{2A_3^2\rho_{g1}p_1\left[\frac{n}{n-1}\left(1-p_r{}^{\frac{n-1}{n}}\right)+\alpha\left(1-p_r\right)\right]}{x_g\left[p_r{}^{-\frac{1}{n}}+\alpha\right]^2\left(1-\left(\frac{[1+\alpha]}{\left[p_r{}^{-\frac{1}{n}}+\alpha\right]}\right)^2\left(\frac{A_3}{A_1}\right)^2\right)\left[x_g+\frac{x_l}{R}\right]} \tag{B.24}$$

With the assumption that $\frac{A_3}{A_1} \ll 1$, $\left(\frac{A_3}{A_1}\right)^2 \approx 0$, together with the introduction of a discharge coefficient C_d to account for the contraction effect and for the irreversible losses in the restriction. The definitive simplified expression for the mass flow rate in sub-critical flow behavior is obtained:

$$\dot{m} = C_d A_3\sqrt{\frac{2\rho_{g1}p_1\left[\frac{n}{n-1}\left(1-p_r{}^{\frac{n-1}{n}}\right)+\alpha\left(1-p_r\right)\right]}{x_g\left[p_r{}^{-\frac{1}{n}}+\alpha\right]^2\left[x_g+\frac{x_l}{R}\right]}} \tag{B.25}$$

B.4. CRITICAL/ SUB-CRITICAL FLOW BOUNDARY

At critical point $\frac{d}{dp_{r,crit}}\left(\frac{\dot{m}^2 x_g}{2A_3^2\rho_{g1}p_1}\right) = 0$ has to be satisfied. Now, when this derivative using B.24 is found and rearranged, the following implicit formula for p_r is found (source: Al-Safran and Kelkar [38]):

$$p_{r,crit}{}^{\frac{n-1}{n}} = \frac{\alpha(1-p_{r,crit})+\frac{n}{n-1}}{\frac{n}{n-1}+\frac{n}{2}\left(1+\alpha p_{r,crit}^{1/n}\right)^2\left[1-\left(\frac{1-\alpha}{p_{r,crit}^{-\frac{1}{n}}+\alpha}\right)\left(\frac{A_3}{A_1}\right)^2\right]} \tag{B.26}$$

If it is assumed that the choke opening is much smaller than the line diameter $\frac{A_3}{A_1} \ll 1$, the expression can be simplified to:

$$p_{r,crit}{}^{\frac{n-1}{n}} = \frac{\alpha(1-p_{r,crit})+\frac{n}{n-1}}{\frac{n}{n-1}+\frac{n}{2}\left(1+\alpha p_{r,crit}^{1/n}\right)^2} \tag{B.27}$$

This expression has to be solved by iteration as it is an implicit expression, in order to define the critical/sub-critical flow boundary.

B.5. CRITICAL MASS FLOW RATE

In the case of the pressure ratio being higher than the critical pressure ratio: $p_r > p_{r,crit}$, $p_r = \frac{p_3}{p_1}$, critical flow through the choke can be assumed. In other words, there is no communication expected backwards through the choke. In this case, of critical flow conditions, equation B.25 should also be used. However, instead of the pressure ratio p_r as input, $p_{r,crit}$ needs to be used, which is calculated implicitly with equation B.27.

C

RESULTS SIGNAL ANALYSIS

The proposed algorithm (the 3 logic tests) in chapter 4 is tested on several production tests. These tests are selected because of their unique characteristic behavior with respect to each other. The results are compared to ad-hoc methods currently used in the industry.

The algorithm is tested on the following production test cases, selected from a database of 700 available production test data sets with Vx meter data:

1. Clear stable flow.
2. Moderate high-frequency random variations.
3. Large high frequency random variations
4. High frequency slugging.
5. Intermittent regimes.
6. Flow regime transition with small random flow behavior

C.1. CASE 1: CLEAR STABLE FLOW

The base case is a very stable flow. This case represents a dispersed or separated flow regime. As there is no fluctuation at all. See figure C.1 the liquid fraction to get a better feeling with the production test characteristics.

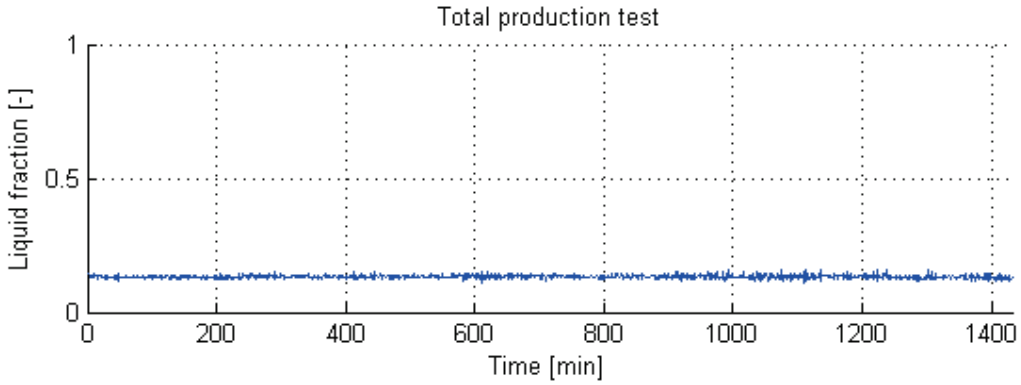

Figure C.1: Case 1. Liquid fraction over the whole production test.

Test 1: Frequency analysis Test one in figure C.2 shows a very flat frequency domain in the 0 to 2 cycles per hour range, under 2000 frequency components. This indicates almost no deviation at all of the signal, test 1 indicates a stable flow.

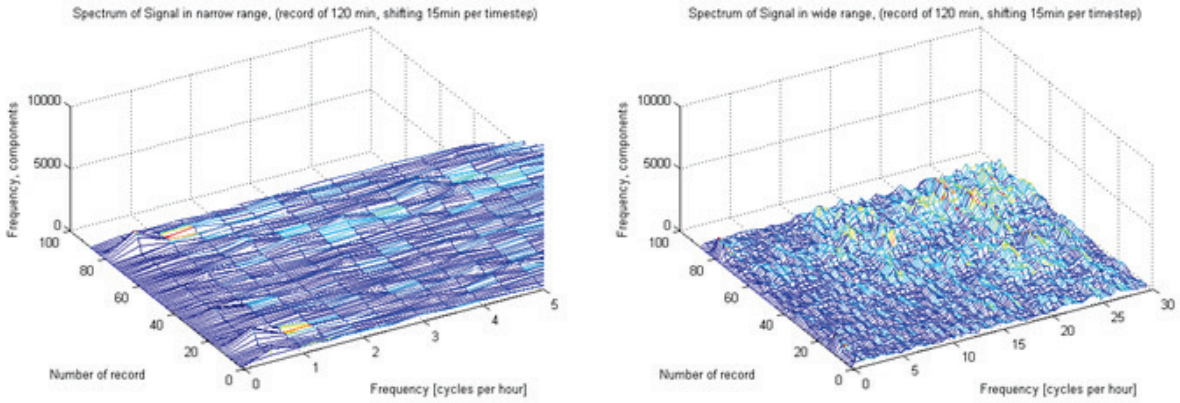

Figure C.2: Test 1 & 3 performed on case 1.

Test 2: PDF analysis The PDF over time and the peaks of the PDF are very constant over time for both the N81 and DPV signal. The difference over time is at all times below the requested 2% for the N81 and 5% for the DPV signal.

Test 3: Slug flow detection The frequency over time in figure C.2 shows no strong peak in the 2 to 10 cycles per hour range. Hence, no slug flow is present.

Conclusion The whole production test is declared stable flow.

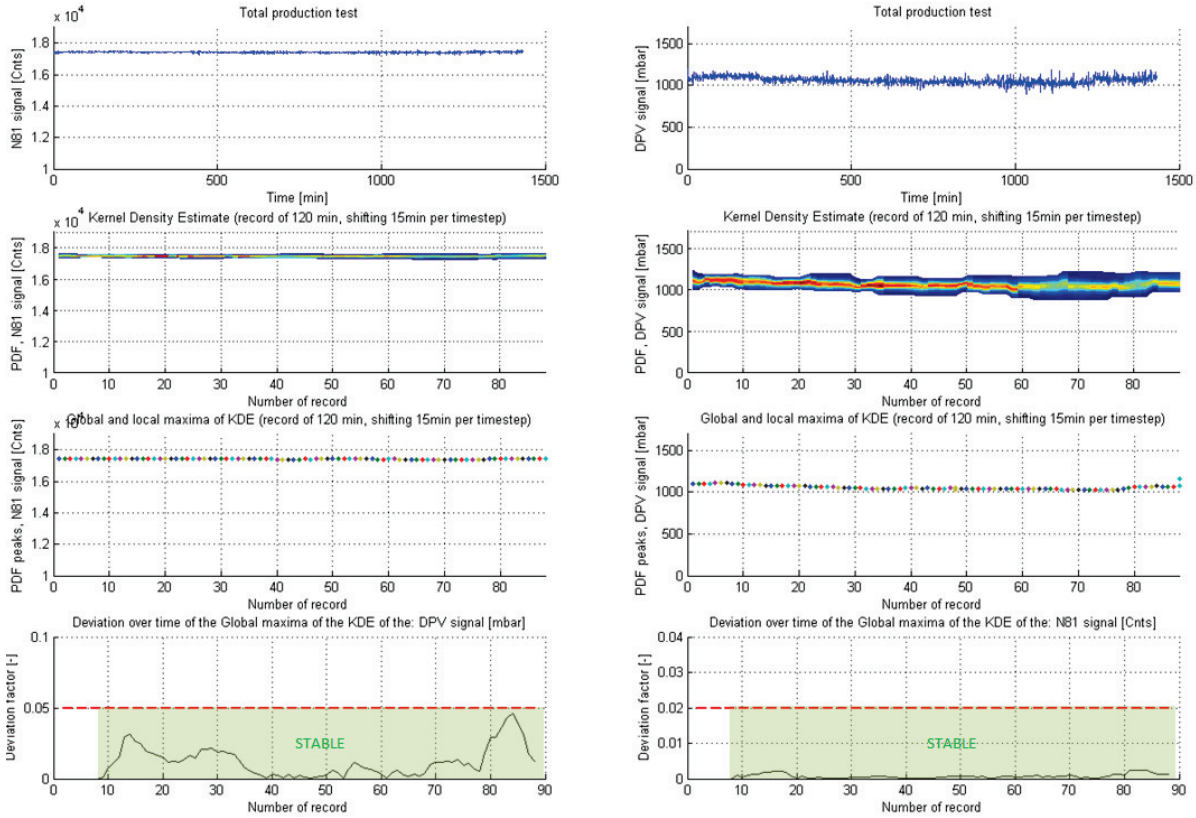

Figure C.3: Test 2 performed on case 1.

C.2. CASE 2: MODERATE HIGH-FREQUENCY RANDOM VARIATIONS

This is a stable case, as the characteristic responses of the signal does not seem to deviate over time. However, there are moderate spikes, visible all over the signal, with a high frequency in figure C.4. The flow regime is unknown. Also whether a stable flow is established is not entirely sure.

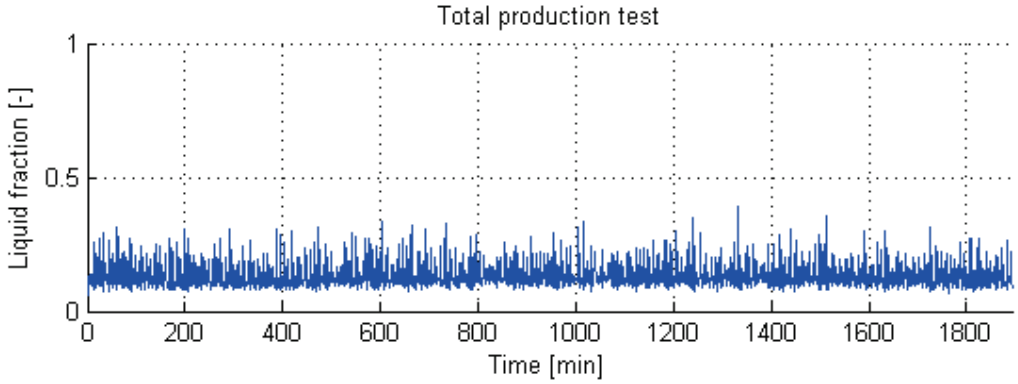

Figure C.4: Case 2. Liquid fraction over the whole production test.

Test 1: Frequency analysis Test one in figure C.5 shows a very flat frequency domain in the 0 to 2 cycles per hour range, below 2000 frequency components. This indicates no deviation at all in the signal. test 1 indicates a stable flow.

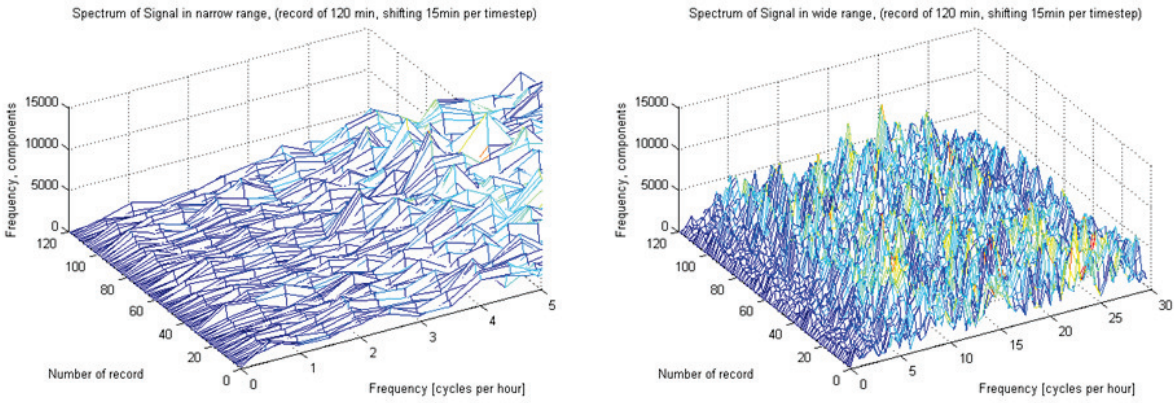

Figure C.5: Test 1 & 3 performed on case 2.

Test 2: PDF analysis The PDF over time and the peaks of the PDF are very constant over time for both the N81 and DPV signal. The PDF is bimodal at several points in time which indicates an intermittent flow regime. The difference over time is at all times below the requested 2% for the N81. The DPV signal is below 5% between timestep 35 and 105.

Test 3: Slug flow detection The frequency over time in figure C.5 shows a lot of small peaks in the 2 to 10 cycles per hour range. This indicates an intermittent flow. However, there are no clear peaks surpassing 10.000 components so no slug flow is present. Most likely there is annalar or a churn flow present.

Conclusion The whole production test is declared an intermittent stable flow from timestep 15 to 29 and from 37 to 105. This is between the 225^{th} and 435^{th} and between the 555^{th} and 1575^{th} minute. This means that the test could have been concluded in the 4th hour of the test.

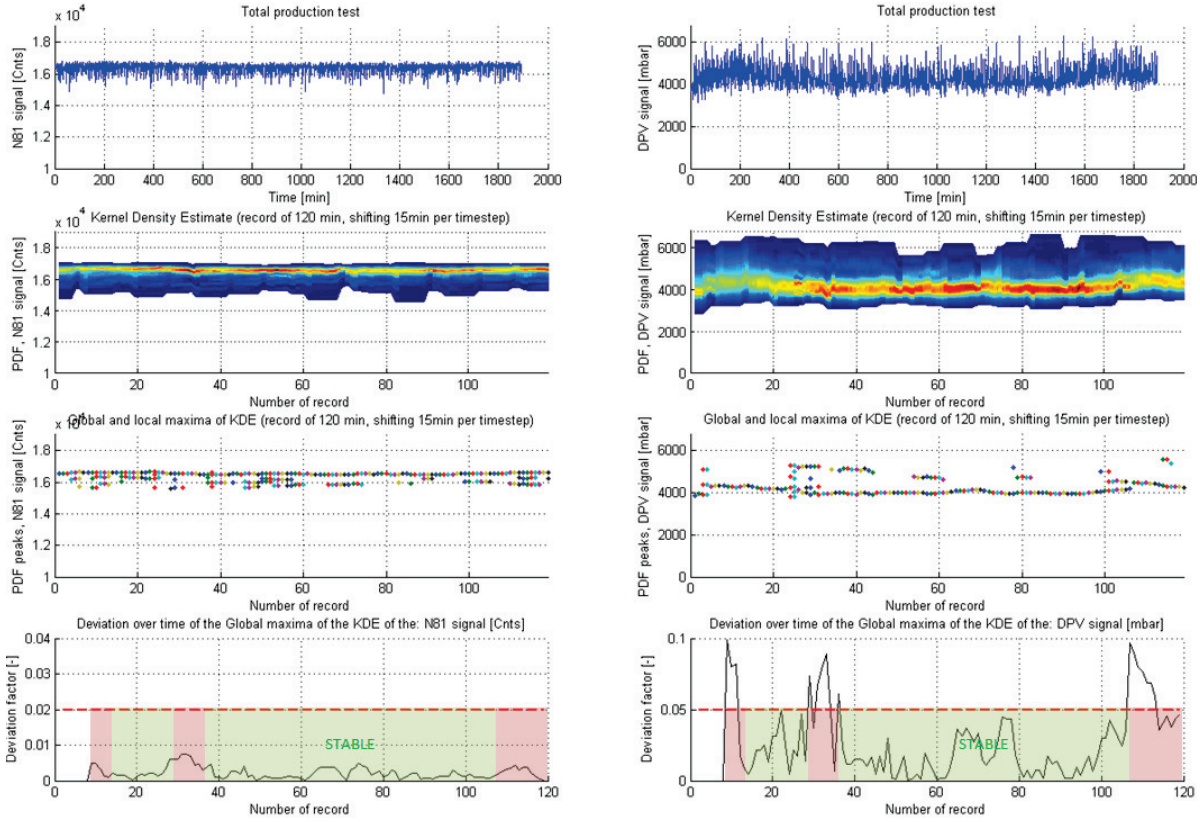

Figure C.6: Test 2 performed on case 2.

C.3. CASE 3: LARGE HIGH-FREQUENCY RANDOM VARIATIONS

Case 3 represents a good example of a complete question-mark concerning the flow stability. The signal is deviating over time and it is uncertain if there is an established flow pattern. In figure C.7 a high-frequency with a random variation is clearly visible.

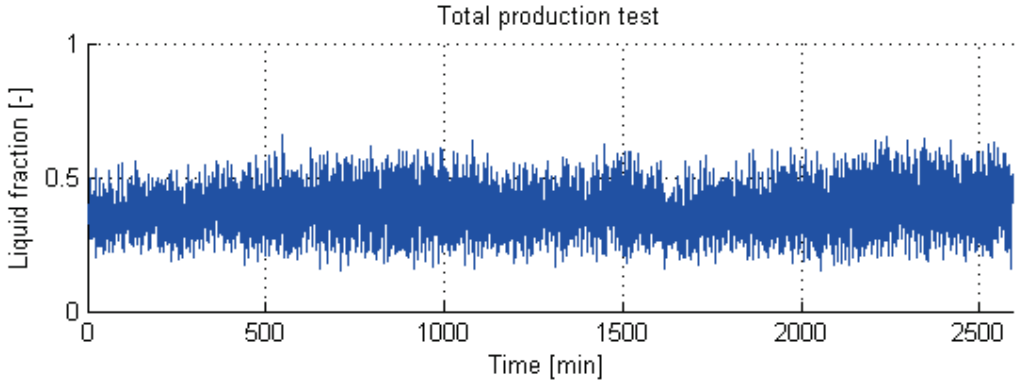

Figure C.7: Case 3. Liquid fraction over the whole production test.

Test 1: Frequency analysis Figure C.8 shows a flat frequency domain in the narrow spectrum, the amount of frequency components are below the requested threshold of 2000. This tells us that the signal can be declared stable as no clear low frequencies are present.

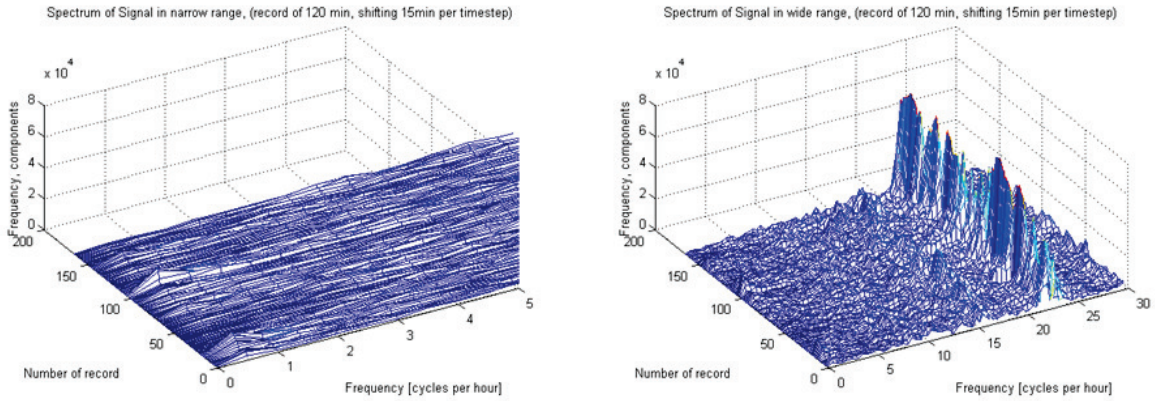

Figure C.8: Test 1 & 3 performed on case 3.

Test 2: PDF analysis The PDF analysis on the signal (figure C.9 shows the behavior of the signal very well. In the third graph, at several timesteps two peaks are visible. So the PDF has a bimodal distribution here which indicates a churn or slug flow. However, the PDF is not constantly bimodal which demonstrates a transitional flow regime. Furthermore, The peaks are not constant all the time. Analysis of the fluctuation of peaks over time shows that the difference is below the required threshold between timestep 30 and 72.

Test 3: Slug flow detection Test 2 points towards an intermittent flow within two flow regimes (transitional flow regime). Test 3 shows clearly that this is not the case. All the large frequency peaks are in the high frequency domain which represents noise, this illustrate that the flow regime is not the origin of the fluctuations in the signal.

Conclusion The whole production test is declared an intermittent stable flow between timestep 30 and 72. This is between the 450th and 1080^{th} minute. The test could have been concluded in the 8th hour of the test.

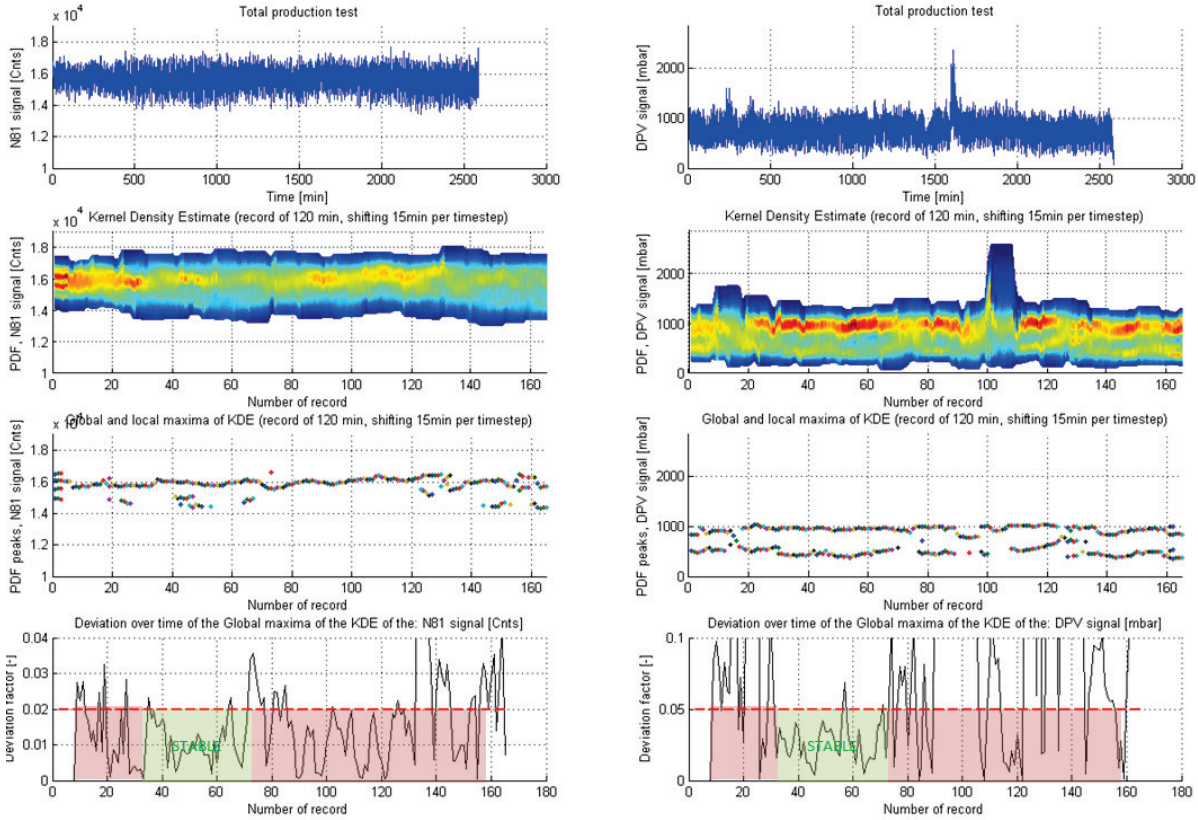

Figure C.9: Test 2 performed on case 3.

C.4. CASE 4: HIGH-FREQUENCY SLUGGING

This case represents a beautiful high frequency slugging case. The signal in figure C.10 shows a lot of fluctuation. With current ad-hoc interpretation methods it would probably be analyzed in the same way as for example Case 2. However, this production test is completely different.

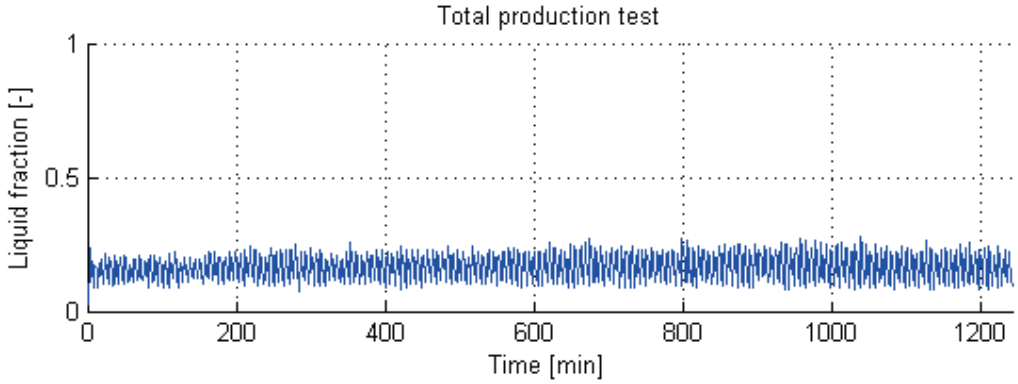

Figure C.10: Case 4. Liquid fraction over the whole production test.

Test 1: Frequency analysis Test 1 shows a very flat frequency domain below 2 cycles per hour, see figureC.11. this tells us that the singal is not deviating over time.

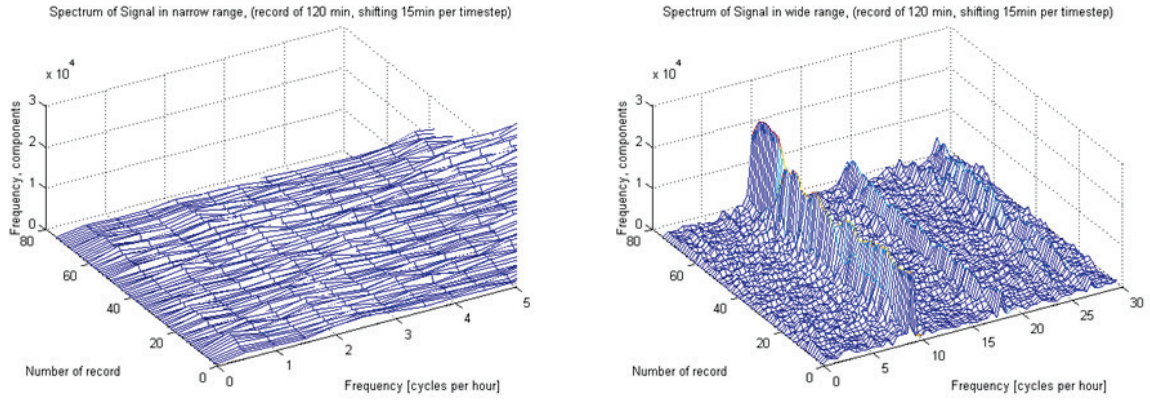

Figure C.11: Test 1 & 3 performed on case 4.

Test 2: PDF analysis Despite all the fluctuations of the signal, the DPV shows us that the stochastical distribution of the signal is very constant over time. The difference of the peaks stay below the required threshold except for one spike in the DPV signal,probably induced by some unique event.

Test 3: Slug flow detection In a case like this Test 3 comes in very useful. There is clearly one spike in the narrow frequency domain above the required threshold of 10.000 components. Figure C.11 shows clearly that the frequency spike is constant as well. This clearly proves that a slug flow regime of 9 slugs per hour is present.

Conclusion The tests show very clearly that this production test was stable for the whole period, exept for some events later on in the production test. It could have been concluded from timestep 15, the 225th minute.

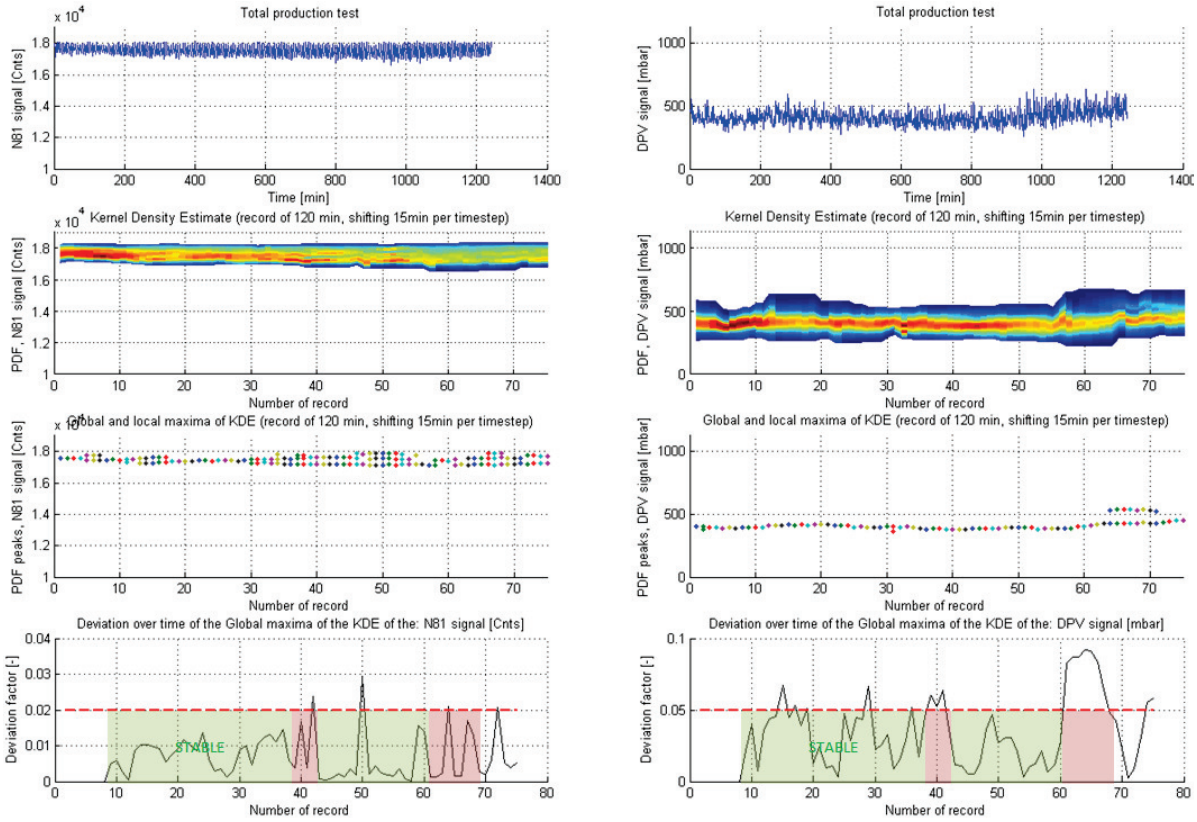

Figure C.12: Test 2 performed on case 4.

C.5. CASE 5: FLOW REGIME TRANSITION WITH RANDOM INTERMITTENT FLOW

Case 5 is an exceptional case which does not occur often. It is included for the sake of completeness.

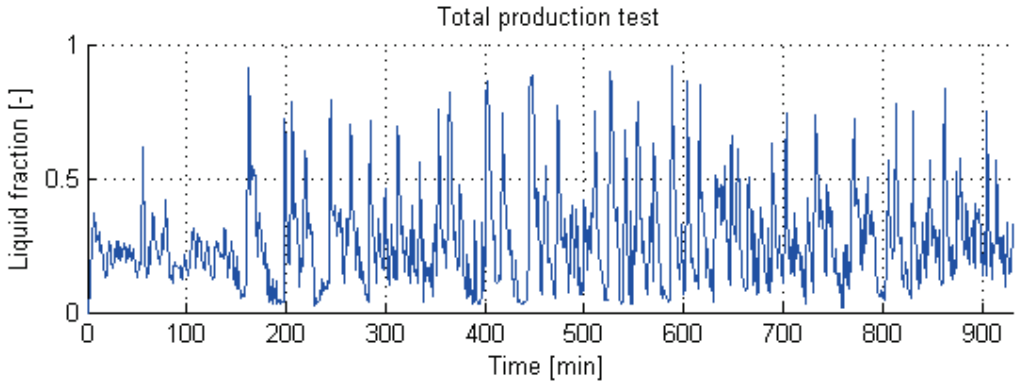

Figure C.13: Case 5. Liquid fraction over the whole production test.

Test 1: Frequency analysis The flow is declared instable according to test 1. it is clearly shown that the frequency surpass the required threshold of 2000 components in the 0 to 2 cycles per hour range. See figure C.14.

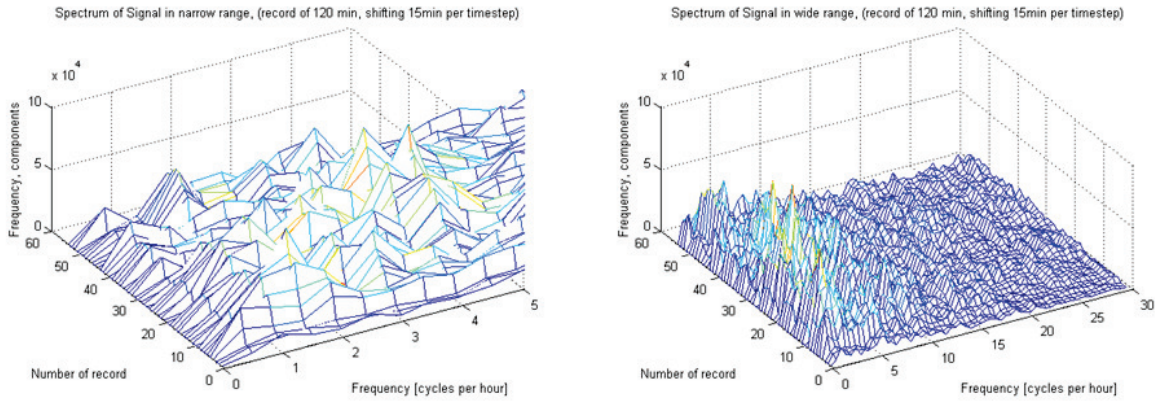

Figure C.14: Test 1 & 3 performed on case 5.

Test 2: PDF analysis The PDF over time in figure C.15 show clearly that the flow regime is constantly changing over the whole production test. Also a bimodal distribution is observed what indicates sluggy behaviour. The DPV signal PDF peak difference is above the requested threshold at all times. Therefore, test 2 declares the flow instable.

Test 3: Slug flow detection Test 3 confirms the suspission of a slug flow regime. Almost the whole narrow frequency domain is above the required threshold of 10.000 componenets. However, The peaks are not constant over time such as in case 4. So a non-constant slug flow.

Conclusion This production test is declared unstable at all times. The test algorithms shows clearly that the flow regime keeps changing over time. The reason for this failed test is the lack of productivity. It is shown in the DPV graphs that the differential pressure at times is approaching zero and that the well has very low productivity, with the unstable flow being a consequence of fluid accumulation in the surface production layout.

With the whole test declared unstable an extra prove is given in figure C.16, here the filtered low frequency is shown in the red line. This line should be a very straight horizontal line in the case of a stable flow. The result in the graph represents that this is clearly not the case throughout the whole signal.

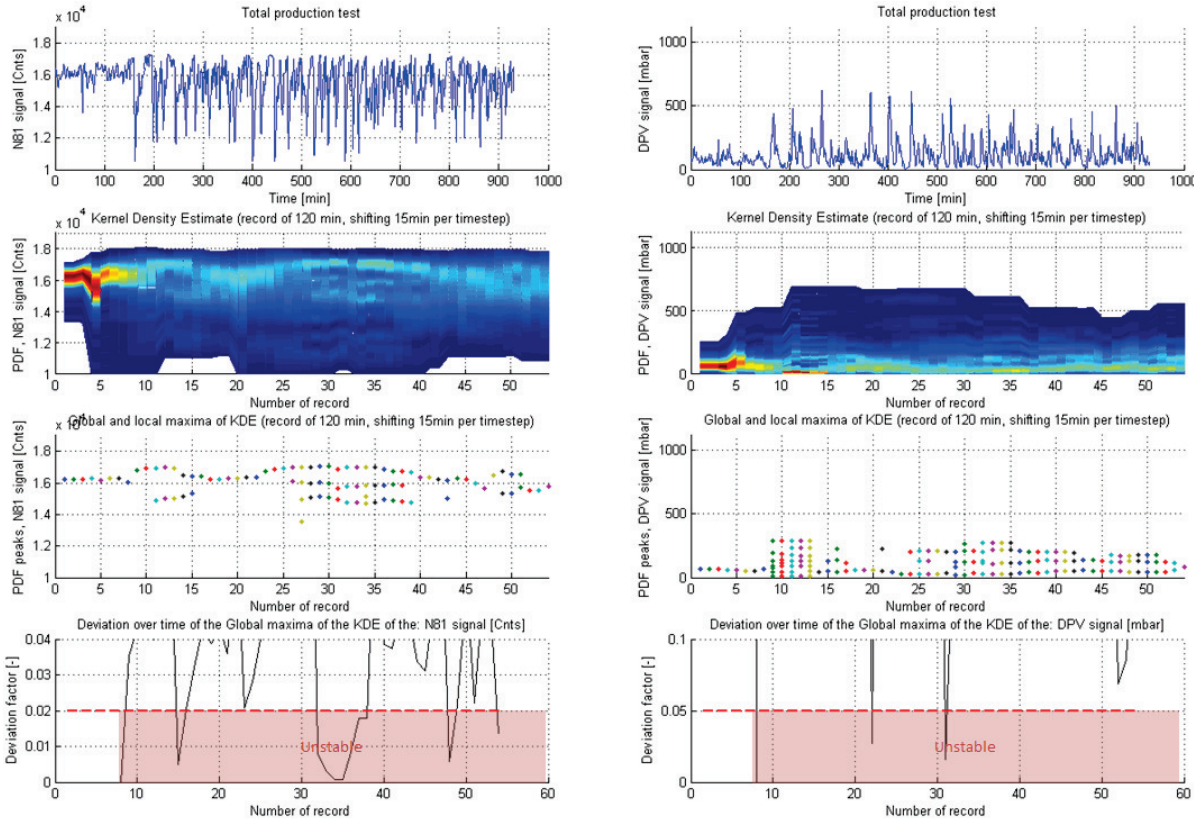

Figure C.15: Test 2 performed on case 5.

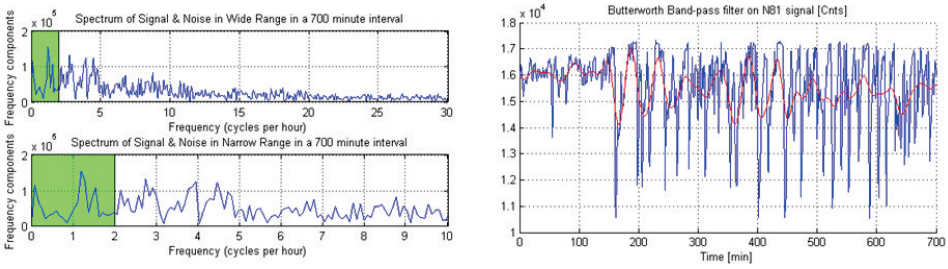

Figure C.16: Band filter on low frequency part of N81 signal. The green area represents what part of the frequency is filtered in order to obtain the red filtered signal.

C.6. CASE 6: FLOW REGIME TRANSITION WITH SMALL RANDOM FLOW BEHAVIOR

Again a production test with a fluctuating signal at high frequency. With an interesting transition in the first part of the production test.

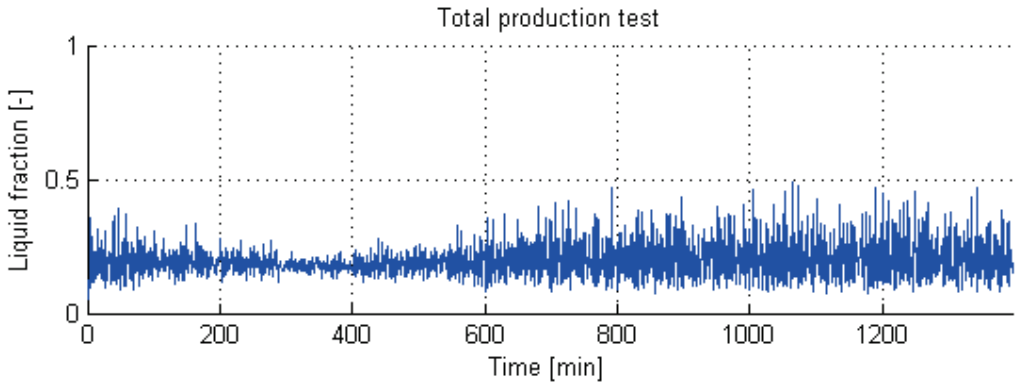

Figure C.17: Case 6. Liquid fraction over the whole production test.

Test 1: Frequency analysis Test 1 in figure C.18 shows a nice flat frequency domain, so there is no deviation on the total production test.

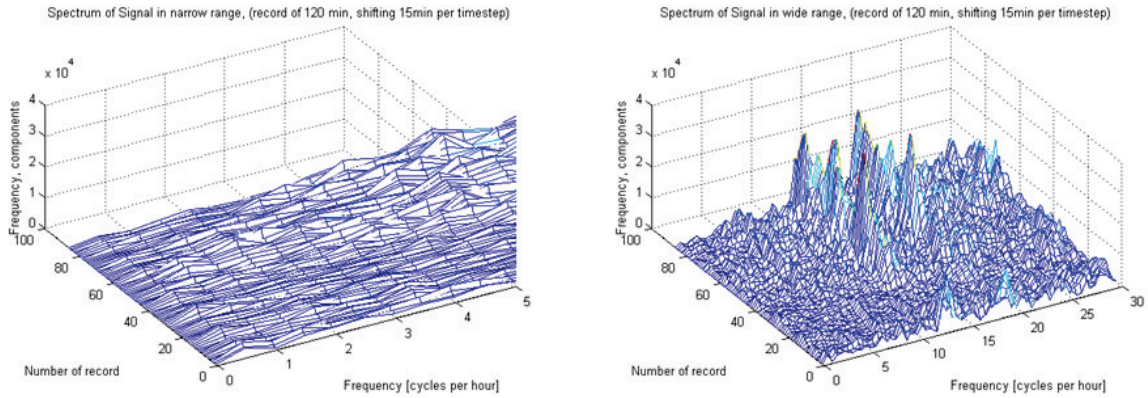

Figure C.18: Test 1 & 3 performed on case 6.

Test 2: PDF analysis From the source signal it was already visible that something was happening in the beginning of the test. The PDF analysis shows in detail where the flow regime is changing and where it is constant. In the second part the PDF distribution becomes bimodal which gives a hint of a churny flow. The DPV signal is below the required threshold from step 50 and on.

Test 3: Slug flow detection There are no peaks in the narrow frequency domain surpassing the 10.000 components, see figure C.18. So all the fluctuation are very high frequency, which implies noise. So the flow regime has no influence on those fluctuations.

Conclusion According to the DPV signal in test 2 this production test is declared stable from time-step 19 to 26 and some other intervals later on. So the production test could have been concluded after 360 minutes.

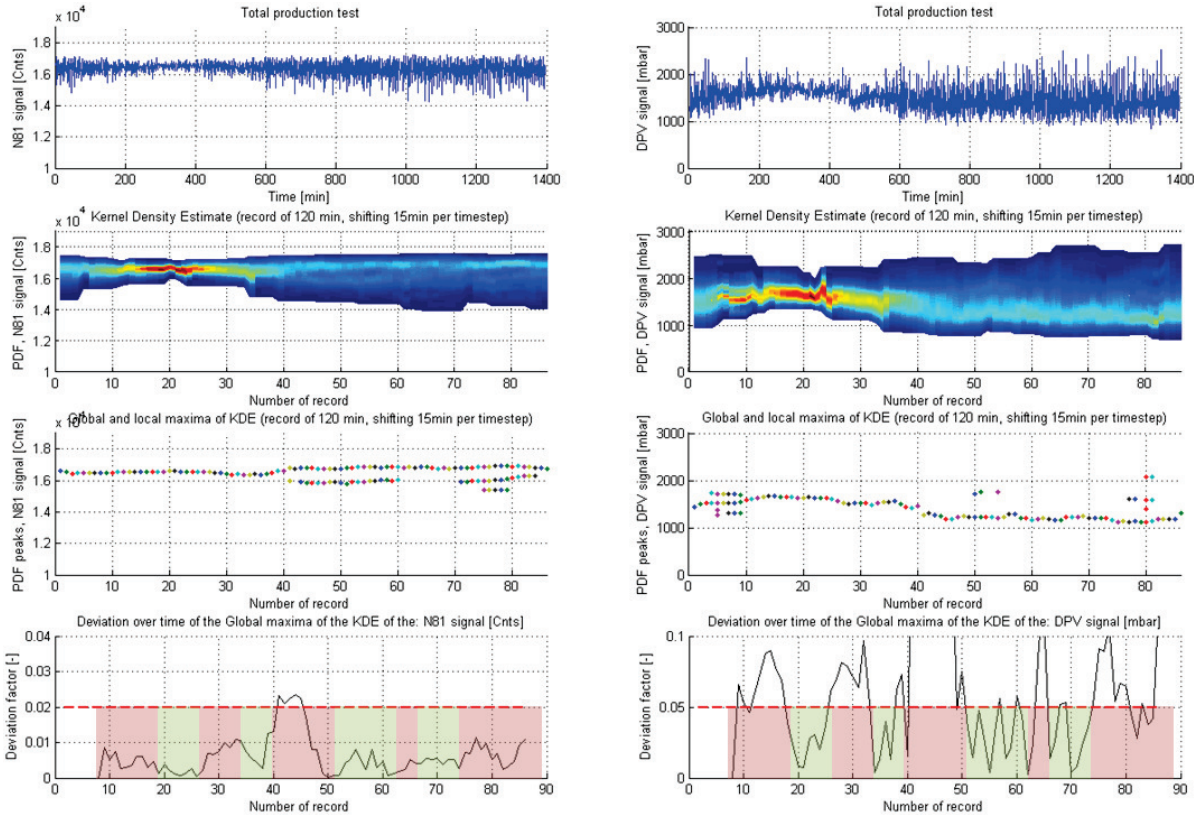

Figure C.19: Test 2 performed on case 6.

BIBLIOGRAPHY

[1] R. W. Miller, *Flow Measurement Engineering Handbook*, 3rd ed. (McGraw-Hill, New York, 1996).

[2] S. Corneliussen, J.-P. Couput, E. Dahl, E. Dykesteen, K.-E. Froysa, E. Malde, H. Moestue, P. O. Mksnes, L. Scheers, and H. Turnheim, *Handbook of Multiphase Flow Metering*, revision 2 ed. (NFOGM & TEKNA, 2005).

[3] A. S. Sikandar, A. Badr, Y. A. Shumakov, B. C. Theuveny, M. McMillon, S. Sarac, and A. G. Fuentes, *Remote real time well testing - experience in the grove gas field in the north sea,* (2010).

[4] A. S. Sikandar, Y. A. Shumakov, S. Sarac, and G. Hetherington, *Putting an end to 'succesful failures',* E&P **March** (2012).

[5] K. I. Ojukwu and J. Edwards, *Reliability of multiphase flowmeters and test separators at high water cut,* (2008) pp. 39–47, export Date: 5 February 2014 Source: Scopus.

[6] B. Theuveny and P. Mehdizadeh, *Multiphase flowmeter applicaton for well and fiscal allocation,* (2002).

[7] B. V. Liddell, D. F. Deaton, and G. Mijares, *Benchmarking measurement and automation practices in the upstream business,* SPE Projects, Facilities and Construction (2007).

[8] G. Falcone, G. F. Hewitt, and C. Alimonti, *Multiphase Flow Metering*, 1st ed., Developments in Petroleum Science (Elsevier, Amsterdam, 2010).

[9] B. Theuveny, S. Valery, R. Konstantin, A. Vitaliy, N. Marat, S. Rustem, and S. Romashkin, *Multiphase metering in siberian gas and condensate fields - lessons leant in multiphase well testing operations since 2006,* (2009).

[10] S. Jayawardane and B. Theuveny, *Pvt sampling with multiphase flowmeters-theoretical justifications and field limitations,* (2002).

[11] F. Hollaender, J. J. Zhang, B. Pinguet, V. Bastos, and E. Delvaux, *An innovative multiphase sampling solution at the well site to improve multiphase flow measurements and phase behavior characterization,* (2007) pp. 1292–1302, export Date: 5 February 2014 Source: Scopus.

[12] Y. A. Shumakov, B. Theuveny, and I. A. Zinchenko, *Field validation processes for multiphase wet gas surface well testing solutions: Example from the yamburgskoe arctic gas condensate field, russia,* (2008).

[13] B. Theuveny, G. Ségéral, Schlumberger, and P. O. Moksnes, *Detection and identification of scales using dual energy / venturi subsea or topside multiphase flow meters,* (2001).

[14] M. Henry, *Self-validation improves coriolis flowmeter,* Control Engineering **42**, 81 (1995), cited By (since 1996):11 Export Date: 12 January 2014 Source: Scopus Language of Original Document: English.

[15] M. Henry, D. W. Clarke, N. Archer, J. Bowles, M. J. Leahy, R. P. Liu, J. Vignos, and F. B. Zhou, *A self-validating digital coriolis mass-flow meter: An overview,* Control Engineering Practice **8**, 487 (2000), cited By (since 1996):60 Export Date: 5 February 2014 Source: Scopus.

[16] M. Al-Saqabi, K. Kahali, and I. M. Al-Kandari, *Evaluation of coriolis meters and gas flow computers for well testing,* , 725 (2000), export Date: 5 February 2014 Source: Scopus Art. No.: SPE 88743.

[17] A. Lomukhin, S. Romashkin, K. Rymarenko, and V. Afanasiyev, *Experience of multiphase flow measurement systems application in arctic conditions,* (2011).

[18] M. N. Al-Khamis, A. F. Al Bassam, Z. Bakhteyar, and M. N. Aftab, *Evaluation of phasewatcher multiphase flow meter (mpfm) performance in sour environments,* (2008).

[19] J. P. Couput, A. Louis, and J. Danquigny, *Transforming e&p data into knowledge: Applications of an integration strategy,* (2008) pp. 1171–1174, export Date: 11 February 2014 Source: Scopus.

[20] J. P. Couput, R. Caulier, and U. Wising, *Field and installation monitoring using on line data validation and reconciliation- application to offshore fields in middle east and west africa,* (2010) pp. 1064–1069, export Date: 5 February 2014 Source: Scopus.

[21] M. Haouche, A. Tessier, Y. Deffous, J. F. Authier, J. P. Couput, R. Caulier, and B. Vrielynck, *Smart metering: An online application of data validation and reconciliation approach,* (2012).

[22] A. Y. Petukhov, L. A. Saputelli, J. B. Hermann, A. I. Traxler, K. B. Boles, O. Nnaji, B. Vrielynck, and D. Venugopal, *Virtual Metering System Application in the Ceiba Field, Offshore Equatorial Guinea*, Tech. Rep. (2011).

[23] O. O. Duru and R. N. Horne, *Simultaneous interpretation of pressure, temperature, and flow-rate data using bayesian inversion methods,* SPE reservoir evaluation & engineering (2011).

[24] M. A. Al-Amri, F. T. Al-Khelaiwi, and M. S. Al-Kadem, *Advanced utilization of downhole sensors for watercut and flow rate allocation,* (2012) pp. 794–801, export Date: 5 February 2014 Source: Scopus.

[25] S. Caicedo and C. Montoya, *Estimating flow rates based on esp down hole sensor data,* (2012) pp. 504–510, export Date: 5 February 2014 Source: Scopus.

[26] M. Piantanida, A. Mazzoni, A. Tanzi, and B. R. Hope, *Multiphase metering: Experimental results from the analysis of acoustic noise through a choke,* (1998) pp. 429–438, export Date: 5 February 2014 Source: Scopus.

[27] I. Lindsay, B. Stimpson, and A. Corlett, *Advanced interpretation of venturi meter measurements in multiphase flow,* (2001) pp. 1747–1754, cited By (since 1996):1 Export Date: 5 February 2014 Source: Scopus.

[28] J. Quevedo, V. Puig, G. Cembrano, J. Blanch, J. Aguilar, D. Saporta, G. Benito, M. Hedo, and A. Molina, *Validation and reconstruction of flow meter data in the barcelona water distribution network,* Control Engineering Practice **18**, 640 (2010).

[29] T. H. J. J. van der Hagen, *Noise analysis; Basics & Practice*, Tech. Rep. (Summer school of the J.M. Burgerscentrum on experimental techniques in multi-phase flow., 1995).

[30] J. Jansen, *Nodal analysis of oil and gas wells - theory and matlab interpretation,* (2014).

[31] W. Gilbert, *Flowing and gas-lift well performance,* Drilling and Production Practice (1954).

[32] N. C. J. Ros, *An analysis of critical simultaneous gas/liquid flow through a restriction and its application to flowmetering,* Applied Scientific Research **9**, 374 (1960), cited By (since 1996):23 Export Date: 3 April 2014 Source: Scopus.

[33] I. Achong, *Revised bean performance formula for Lake Maracaibo wells*, Tech. Rep. (Shell Oil Company, 1961).

[34] A. Pilehvari, *Experimental study of critical two-phase flow through wellhead chokes*, Ph.D. thesis (1981).

[35] F. E. Ashford and P. E. Pierce, *Determining multiphase pressure drops and flow capacities in down-hole safety valves,* JPT, Journal of Petroleum Technology **27**, 1145 (1975), cited By (since 1996):27 Export Date: 21 July 2014.

[36] M. E. Osman and M. E. Dokla, *Gas condensate flow through chokes,* Society of Petroleum Engineers of AIME, (Paper) SPE (1990), export Date: 21 July 2014.

[37] R. Omana, C. J. Houssiere, K. Brown, J. P. Brill, and R. Thompson, *Multiphase flow through chokes.* Society of Petroleum Engineers of AIME (1969).

[38] E. M. Al-Safran and M. Kelkar, *Predictions of two-phase critical-flow boundary and mass-flow rate across chokes,* SPE Production and Operations **24**, 249 (2009), cited By (since 1996):2 Export Date: 3 April 2014 Source: Scopus.

[39] T. K. Perkins, *Critical and subcritical flow of multiphase mixtures through chokes,* SPE Drilling and Completion **8**, 271 (1993), cited By (since 1996):33 Export Date: 3 April 2014 Source: Scopus.

[40] R. Sachdeva, Z. Schmidt, J. P. Brill, and R. M. Blais, *Two-phase flow through chokes,* (1986), export Date: 3 April 2014 Source: Scopus.

[41] R. B. Schüller, T. Solbakken, and S. Selmer-Olsen, *Evaluation of multiphase flow rate models for chokes under subcritical oil/gas/water flow conditions,* SPE Production and Facilities **18**, 170 (2003), cited By (since 1996):8 Export Date: 3 April 2014 Source: Scopus.

[42] M. Grolmes and S. Coates, *Progress report on High Viscosity Two-Phase Flow Modelling,*, Tech. Rep. (Presentation for 20th DIERS Users Group, 1997).

[43] H. C. Simpson, D. H. Rooney, and E. Grattan, *Two phase flow through gate valves and orifice plates,* , 25 (1983), cited By (since 1996):10 Export Date: 3 April 2014 Source: Scopus.

[44] R. B. Schüller, S. Munaweera, S. Selmer-Olsen, and T. Solbakken, *Critical and subcritical oil/gas/water mass flow rate experiments and predictions for chokes,* SPE Production and Operations **21**, 372 (2006), cited By (since 1996):4 Export Date: 3 April 2014 Source: Scopus.

[45] B. Pinguet, *Fundamentals of Multiphase Flow Metering* (Schlumberger, Sugar Land, 2010).

[46] T. H. J. J. van der Hagen and J. van der Voet, *Interpretation of velocities determined by noise analysis for various void fractions and flow regimes in two-phase flow,* Progress in Nuclear Energy **21**, 565 (1988), cited By (since 1996):1 Export Date: 1 July 2014.

[47] T. H. J. J. Van der Hagen and J. E. Hoogenboom, *Fast measurements of the in-core coolant velocity in a bwr by neutron noise analysis,* Annals of Nuclear Energy **15**, 439 (1988), cited By (since 1996):4 Export Date: 1 July 2014.

[48] Y. K. Suman, T. K. Mandal, and G. Das, *Use of digital signal analysis to identify slug flow in a narrow vertical pipe,* Chemical Engineering Communications **197**, 1287 (2010), export Date: 7 July 2014.

[49] O. C. Jones Jr and N. Zuber, *The interrelation between void fraction fluctuations and flow patterns in two-phase flow,* International Journal of Multiphase Flow **2**, 273 (1975), cited By (since 1996):179 Export Date: 7 July 2014.

[50] O. C. Jones Jr and J. M. Delhaye, *Transient and statistical measurement techniques for two-phase flows: A critical review,* International Journal of Multiphase Flow **3**, 89 (1976), cited By (since 1996):60 Export Date: 7 July 2014.

[51] Z. I. Botev, J. F. Grotowski, and D. P. Kroese, *Kernel density estimation via diffusion,* Annals of Statistics **38**, 2916 (2010), cited By (since 1996):204 Export Date: 15 July 2014.

NOMENCLATURE

Abbreviations

BOM	Black Oil Model
CNF	Configuration file for Vx meter
DPV	Differential pressure sensor in Vx meter
DVR	Data Validation and Reconcilition
ESP	Electric Submersible Pump
GLR	Gas Liquid Ratio
GOR	Gas Oil Ratio
NN	Neural Network
PDG	Permanent Downhole Gauge
VFM	Virtual Flow Meter
WCT	Water cut
WLR	Water Liquid Ratio

Choke model symbols

$\dot{m}$	mass flow rate, kg/s
μ	viscosity, $Pa \cdot s$
ρ	density, kg/m^3
σ	standard deviation, %
A	cross sectional area, m^2
C_d	overall discharge coefficient
c_{pg}	specific heat capacity of liquid at constant pressure
c_{vg}	specific heat capacity of gas at constant volume
c_{vl}	specific heat capacity of liquid at constant volume
d	diameter of section, m
e_1	average percent error, %
e_2	absolute average percent error, %
n	polytropic heat coefficient
p	pressure, Pa
R	slip ratio
x	quality, (or mass fraction)

Subscripts

1	pipe section upstream of choke
2	pipe section at inlet of choke restriction
3	pipe section at outlet of choke restriction
3	pipe section downstream of choke
$crit$	critical
c	choke
g	gas
l	liquid
m	mixture
o	oil
r	ratio, $\frac{3}{1}$
w	water

List of Figures